Suppression of temperature-gradient-driven turbulence by perpendicular flow shear

P. G. Ivanov[1], T. Adkins[1,2], D. Kennedy[3], M. Giacomin[4], A. A. Schekochihin[1], M. Barnes[1]

[1] *Rudolf Peierls Centre for Theoretical Physics, University of Oxford, Oxford, OX1 3PU, United Kingdom*

[2] *Department of Physics, University of Otago, Dunedin, 9016, New Zealand*

[3] *Culham Centre for Fusion Energy, Abingdon OX14 3DB, United Kingdom*

[4] *Dipartimento di Fisica "G. Galilei", Università degli Studi di Padova, Padova, Italy*

Motivation

Motivation

- Understanding and taming turbulence is crucial for designing successful fusion reactors.

Motivation

- Understanding and taming turbulence is crucial for designing successful fusion reactors.
- Both experimental and numerical results confirm that **flow shear suppresses turbulence**.

Motivation

- Understanding and taming turbulence is crucial for designing successful fusion reactors.
- Both experimental and numerical results confirm that **flow shear suppresses turbulence**.
- Sheared flows may be intrinsically generated (e.g., zonal flows) or externally imposed (e.g., equilibrium flow shear).

Motivation

- Understanding and taming turbulence is crucial for designing successful fusion reactors.
- Both experimental and numerical results confirm that **flow shear suppresses turbulence**.
- Sheared flows may be intrinsically generated (e.g., zonal flows) or externally imposed (e.g., equilibrium flow shear).

We want to address the fundamental mechanisms whereby the flow shear regulates the turbulent transport.

Outline

Outline

Gyrokinetics

Nonlinear saturation without flow shear

Adding flow shear

Numerical results

Possible application

Local electrostatic gyrokinetics

$$\left(\frac{\partial}{\partial t} + \boldsymbol{u}\cdot\frac{\partial}{\partial \boldsymbol{R}_s}\right)\left(h_s - \frac{q_s \left\langle \phi \right\rangle_{\boldsymbol{R}_s}}{T_{0s}} f_{0s}\right) + v_{\parallel}\boldsymbol{b}_0\cdot\frac{\partial h_s}{\partial \boldsymbol{R}_s} + \boldsymbol{v}_{ds}\cdot\frac{\partial h_s}{\partial \boldsymbol{R}_s} + \boldsymbol{v}_E\cdot\frac{\partial}{\partial \boldsymbol{R}_s}\left(f_{0s} + h_s\right) = \sum_{s'} C_{ss'}, \tag{1}$$

with

$$\boldsymbol{v}_{ds} = (\boldsymbol{b}_0/2\Omega_s)\times(2w_{\parallel}^2\boldsymbol{b}_0\cdot\boldsymbol{\nabla}\boldsymbol{b}_0 + w_{\perp}^2\boldsymbol{\nabla}\ln B_0), \quad \boldsymbol{v}_E = (c/B_0)\boldsymbol{b}_0\times\boldsymbol{\nabla}\left\langle\phi\right\rangle_{\boldsymbol{R}_s}, \tag{2}$$

the perturbed distribution function of species s is

$$\delta f_s(\boldsymbol{r},\boldsymbol{v}) = h_s(\boldsymbol{R}_s, \varepsilon_s, \mu_s) - \frac{q_s\phi(\boldsymbol{r})}{T_s} f_{0s} \tag{3}$$

and satisfies

$$\sum_s q_s \int \mathrm{d}^3\boldsymbol{v}\, \delta f_s = 0. \tag{4}$$

Local electrostatic gyrokinetics

$$\left(\frac{\partial}{\partial t} + \boldsymbol{u}\cdot\frac{\partial}{\partial \boldsymbol{R}_s}\right)\left(h_s - \frac{q_s\left\langle\phi\right\rangle_{\boldsymbol{R}_s}}{T_{0s}}f_{0s}\right) + v_\parallel \boldsymbol{b}_0\cdot\frac{\partial h_s}{\partial \boldsymbol{R}_s} + \boldsymbol{v}_{ds}\cdot\frac{\partial h_s}{\partial \boldsymbol{R}_s} + \boldsymbol{v}_E\cdot\frac{\partial}{\partial \boldsymbol{R}_s}\left(f_{0s}+h_s\right) = \sum_{s'} C_{ss'}, \tag{1}$$

with

$$\boldsymbol{v}_{ds} = (\boldsymbol{b}_0/2\Omega_s)\times\left(2w_\parallel^2\boldsymbol{b}_0\cdot\boldsymbol{\nabla}\boldsymbol{b}_0 + w_\perp^2\boldsymbol{\nabla}\ln B_0\right), \quad \boldsymbol{v}_E = (c/B_0)\boldsymbol{b}_0\times\boldsymbol{\nabla}\left\langle\phi\right\rangle_{\boldsymbol{R}_s}, \tag{2}$$

the perturbed distribution function of species s is

$$\delta f_s(\boldsymbol{r},\boldsymbol{v}) = h_s(\boldsymbol{R}_s,\varepsilon_s,\mu_s) - \frac{q_s\phi(\boldsymbol{r})}{T_s}f_{0s} \tag{3}$$

and satisfies

$$\sum_s q_s\int \mathrm{d}^3\boldsymbol{v}\,\delta f_s = 0. \tag{4}$$

We shall be interested in predicting the radial heat flux

$$Q_s = \int\frac{\mathrm{d}^3\boldsymbol{r}}{V}\int\mathrm{d}^3\boldsymbol{v}\,\left(\boldsymbol{v}_E\cdot\boldsymbol{\nabla}x\right)\frac{m_s v^2}{2}\delta f_s, \tag{5}$$

where x, y, z are the radial, poloidal, and field-line-following coordinates, respectively.

Free-energy conservation in GK

Free-energy conservation in GK

- GK fluctuations obey the free-energy conservation:

$$\frac{dW}{dt} = I - D \tag{6}$$

Free-energy conservation in GK

- GK fluctuations obey the free-energy conservation:

$$\frac{dW}{dt} = I - D \tag{6}$$

where the free energy W is

$$W = \sum_s \int \mathrm{d}^3\boldsymbol{r} \int \mathrm{d}^3\boldsymbol{v} \frac{T_{0s}\delta f_s^2}{2 f_{0s}}. \tag{7}$$

Free-energy conservation in GK

- GK fluctuations obey the free-energy conservation:

$$\frac{dW}{dt} = I - D \tag{6}$$

where the free energy W is

$$W = \sum_s \int \mathrm{d}^3\boldsymbol{r} \int \mathrm{d}^3\boldsymbol{v}\, \frac{T_{0s}\delta f_s^2}{2f_{0s}}. \tag{7}$$

- I is the energy injection (equilibrium gradients times fluxes), D is collisional dissipation.

Where do we even begin?

Where do we even begin?

Without any additional assumptions, this is hopeless!

Where do we even begin?

Without any additional assumptions, this is hopeless!

- A zoo of instabilities (2×ITG, 2×ETG, TEM, ...)

Where do we even begin?

Without any additional assumptions, this is hopeless!

- A zoo of instabilities (2×ITG, 2×ETG, TEM, ...)
- Many different regimes (strong turbulence, Dimits regime, ...)

Where do we even begin?

Without any additional assumptions, this is hopeless!

- A zoo of instabilities (2×ITG, 2×ETG, TEM, . . .)
- Many different regimes (strong turbulence, Dimits regime, . . .)
- Zonal flows, secondary instabilities, tertiary instabilities, . . .

Where do we even begin?

Without any additional assumptions, this is hopeless!

- A zoo of instabilities ($2\times$ITG, $2\times$ETG, TEM, ...)
- Many different regimes (strong turbulence, Dimits regime, ...)
- Zonal flows, secondary instabilities, tertiary instabilities, ...

Main conjecture: Saturation is achieved by establishing a cascade of free energy from the injection scale to the dissipation scale.

Where do we even begin?

Without any additional assumptions, this is hopeless!

- A zoo of instabilities (2×ITG, 2×ETG, TEM, . . .)
- Many different regimes (strong turbulence, Dimits regime, . . .)
- Zonal flows, secondary instabilities, tertiary instabilities, . . .

Main conjecture: Saturation is achieved by establishing a cascade of free energy from the injection scale to the dissipation scale.

- Not unreasonable, happens in, e.g., hydrodynamics (Kolmogorov, 1941) and MHD (Goldreich & Sridhar, 1995).

Where do we even begin?

Without any additional assumptions, this is hopeless!

- A zoo of instabilities (2×ITG, 2×ETG, TEM, . . .)
- Many different regimes (strong turbulence, Dimits regime, . . .)
- Zonal flows, secondary instabilities, tertiary instabilities, . . .

Main conjecture: Saturation is achieved by establishing a cascade of free energy from the injection scale to the dissipation scale.

- Not unreasonable, happens in, e.g., hydrodynamics (Kolmogorov, 1941) and MHD (Goldreich & Sridhar, 1995).
- Observed by Barnes et al. (2011) in ion-scale turbulence (some aspects challenged by more recent observations by Nies et al., 2023), and Adkins et al. (2023) in electron-scale fluid turbulence.

Outline

Gyrokinetics

Nonlinear saturation without flow shear

Adding flow shear

Numerical results

Possible application

Local energy cascade

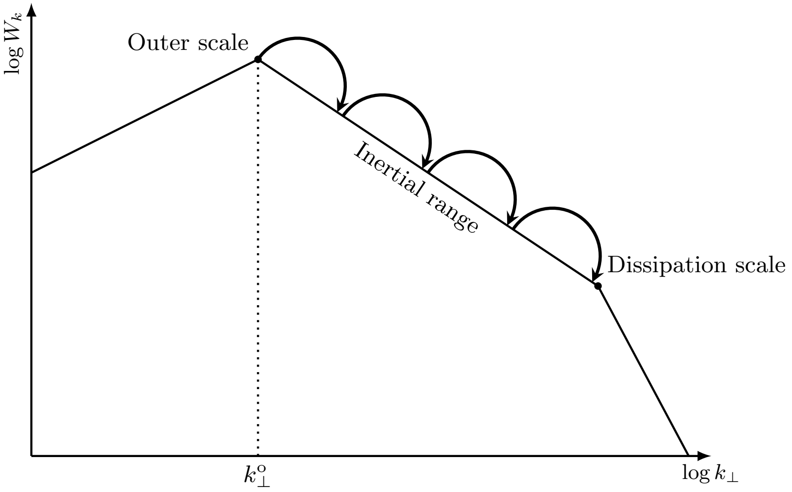

Local energy cascade

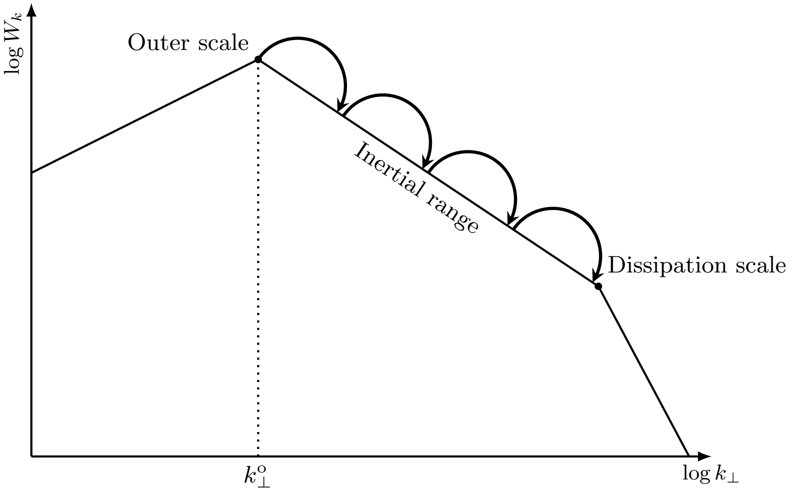

- **In the inertial range, nonlinear interactions dominate every other source/sink of energy.**

Inertial range

- The nonlinear GK term is
$$\boldsymbol{v}_E \cdot \frac{\partial h_s}{\partial \boldsymbol{R}_s} = \frac{c}{B_0} \left\{ \langle \phi \rangle_{\boldsymbol{R}_s}, h_s \right\}, \tag{8}$$
where $\{f, g\} \propto (\partial_x f)(\partial_y g) - (\partial_y f)(\partial_x g)$,

Inertial range

- The nonlinear GK term is

$$\boldsymbol{v}_E \cdot \frac{\partial h_s}{\partial \boldsymbol{R}_s} = \frac{c}{B_0} \left\{ \langle \phi \rangle_{\boldsymbol{R}_s}, h_s \right\}, \tag{8}$$

where $\{f, g\} \propto (\partial_x f)(\partial_y g) - (\partial_y f)(\partial_x g)$, so the nonlinear time τ_{nl} at scale k_y satisfies

$$\tau_{\mathrm{nl}}^{-1} \sim \Omega_s \rho_s^2 k_x k_y \overline{\varphi}, \tag{9}$$

where $\varphi \equiv q_s \phi / T_{0s}$ and $\overline{\varphi}$ is its **characteristic amplitude** at scale k_y.

Inertial range

- The nonlinear GK term is
$$\boldsymbol{v}_E \cdot \frac{\partial h_s}{\partial \boldsymbol{R}_s} = \frac{c}{B_0} \left\{ \langle \phi \rangle_{\boldsymbol{R}_s}, h_s \right\}, \tag{8}$$
where $\{f, g\} \propto (\partial_x f)(\partial_y g) - (\partial_y f)(\partial_x g)$, so the nonlinear time $\tau_{\rm nl}$ at scale k_y satisfies
$$\tau_{\rm nl}^{-1} \sim \Omega_s \rho_s^2 k_x k_y \overline{\varphi}, \tag{9}$$
where $\varphi \equiv q_s \phi / T_{0s}$ and $\overline{\varphi}$ is its **characteristic amplitude** at scale k_y.
- In (9), k_x and $\overline{\varphi}$ are both functions of k_y.

Inertial range

- The nonlinear GK term is
$$\boldsymbol{v}_E \cdot \frac{\partial h_s}{\partial \boldsymbol{R}_s} = \frac{c}{B_0} \left\{ \langle \phi \rangle_{\boldsymbol{R}_s}, h_s \right\}, \tag{8}$$
where $\{f, g\} \propto (\partial_x f)(\partial_y g) - (\partial_y f)(\partial_x g)$, so the nonlinear time $\tau_{\rm nl}$ at scale k_y satisfies
$$\tau_{\rm nl}^{-1} \sim \Omega_s \rho_s^2 k_x k_y \overline{\varphi}, \tag{9}$$
where $\varphi \equiv q_s \phi / T_{0s}$ and $\overline{\varphi}$ is its **characteristic amplitude** at scale k_y.
- In (9), k_x and $\overline{\varphi}$ are both functions of k_y.
- Rewrite as
$$\tau_{\rm nl}^{-1} \sim \mathcal{A} \Omega_s \rho_s^2 k_y^2 \overline{\varphi}, \tag{10}$$
where $\mathcal{A} \equiv k_x / k_y$ is the **fluctuation aspect ratio** at scale k_y.

Inertial range

- The nonlinear GK term is
$$\boldsymbol{v}_E \cdot \frac{\partial h_s}{\partial \boldsymbol{R}_s} = \frac{c}{B_0}\left\{\langle\phi\rangle_{\boldsymbol{R}_s}, h_s\right\}, \tag{8}$$
where $\{f, g\} \propto (\partial_x f)(\partial_y g) - (\partial_y f)(\partial_x g)$, so the nonlinear time τ_{nl} at scale k_y satisfies
$$\tau_{\mathrm{nl}}^{-1} \sim \Omega_s \rho_s^2 k_x k_y \overline{\varphi}, \tag{9}$$
where $\varphi \equiv q_s\phi/T_{0s}$ and $\overline{\varphi}$ is its **characteristic amplitude** at scale k_y.
- In (9), k_x and $\overline{\varphi}$ are both functions of k_y.
- Rewrite as
$$\tau_{\mathrm{nl}}^{-1} \sim \mathcal{A}\Omega_s \rho_s^2 k_y^2 \overline{\varphi}, \tag{10}$$
where $\mathcal{A} \equiv k_x/k_y$ is the **fluctuation aspect ratio** at scale k_y.

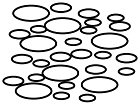

$\mathcal{A} < 1$

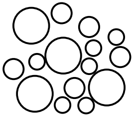

$\mathcal{A} \sim 1$

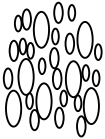

$\mathcal{A} > 1$

The isotropic energy cascade

- Assuming an isotropic cascade, $\mathcal{A} \sim 1$ and

$$\tau_{\mathrm{nl}}^{-1} \sim \mathcal{A}\Omega_s \rho_s^2 k_y^2 \overline{\varphi} \propto k_\perp^2 \overline{\varphi}. \tag{11}$$

The isotropic energy cascade

- Assuming an isotropic cascade, $\mathcal{A} \sim 1$ and

$$\tau_{\mathrm{nl}}^{-1} \sim \mathcal{A}\Omega_s \rho_s^2 k_y^2 \overline{\varphi} \propto k_\perp^2 \overline{\varphi}. \tag{11}$$

- The flux of free energy ε through each scale $k_\perp$ satisfies

$$\varepsilon \sim \overline{W} \tau_{\mathrm{nl}}^{-1} \sim n_{0s} T_{0s} \overline{\varphi}^2 \tau_{\mathrm{nl}}^{-1}$$

The isotropic energy cascade

- Assuming an isotropic cascade, $\mathcal{A} \sim 1$ and

$$\tau_{\mathrm{nl}}^{-1} \sim \mathcal{A}\Omega_s \rho_s^2 k_y^2 \overline{\varphi} \propto k_\perp^2 \overline{\varphi}. \tag{11}$$

- The flux of free energy ε through each scale $k_\perp$ satisfies

$$\varepsilon \sim \overline{W}\tau_{\mathrm{nl}}^{-1} \sim n_{0s} T_{0s} \overline{\varphi}^2 \tau_{\mathrm{nl}}^{-1} \propto k_\perp^2 \overline{\varphi}^3. \tag{12}$$

The isotropic energy cascade

- Assuming an isotropic cascade, $\mathcal{A} \sim 1$ and

$$\tau_{\mathrm{nl}}^{-1} \sim \mathcal{A}\Omega_s \rho_s^2 k_y^2 \overline{\varphi} \propto k_\perp^2 \overline{\varphi}. \tag{11}$$

- The flux of free energy ε through each scale $k_\perp$ satisfies

$$\varepsilon \sim \overline{W}\tau_{\mathrm{nl}}^{-1} \sim n_{0s} T_{0s} \overline{\varphi}^2 \tau_{\mathrm{nl}}^{-1} \propto k_\perp^2 \overline{\varphi}^3. \tag{12}$$

- A constant ε in the inertial range implies

$$\overline{\varphi} \propto k_\perp^{-2/3} \implies \tau_{\mathrm{nl}}^{-1} \propto k_\perp^{4/3}. \tag{13}$$

But where does the inertial range start?

But where does the inertial range start?

- Injection of energy is done by linear instabilities.

But where does the inertial range start?

- Injection of energy is done by linear instabilities.
- At large scales, the growth rate of the most unstable modes (usually) satisfies $\gamma_{\boldsymbol{k}} \propto k_y$.

But where does the inertial range start?

- Injection of energy is done by linear instabilities.
- At large scales, the growth rate of the most unstable modes (usually) satisfies $\gamma_{\boldsymbol{k}} \propto k_y$.
- The outer scale $\boldsymbol{k}^{\mathrm{o}}$ is the scale where

$$\gamma^{\mathrm{o}} \sim {\tau_{\mathrm{nl}}^{\mathrm{o}}}^{-1}. \tag{14}$$

But where does the inertial range start?

- Injection of energy is done by linear instabilities.
- At large scales, the growth rate of the most unstable modes (usually) satisfies $\gamma_{\boldsymbol{k}} \propto k_y$.
- The outer scale $\boldsymbol{k}^{\mathrm{o}}$ is the scale where

$$\gamma^{\mathrm{o}} \sim {\tau_{\mathrm{nl}}^{\mathrm{o}}}^{-1}. \tag{14}$$

This is where the dominant injection of energy happens.

But where does the inertial range start?

- Injection of energy is done by linear instabilities.
- At large scales, the growth rate of the most unstable modes (usually) satisfies $\gamma_{\boldsymbol{k}} \propto k_y$.
- The outer scale $\boldsymbol{k}^{\mathrm{o}}$ is the scale where

$$\gamma^{\mathrm{o}} \sim \tau_{\mathrm{nl}}^{\mathrm{o}\,-1}. \tag{14}$$

  This is where the dominant injection of energy happens.
- Beyond the outer scale, nonlinearity dominates as $\tau_{\mathrm{nl}}^{-1} \propto k_{\perp}^{4/3} \gg \gamma_{\boldsymbol{k}} \sim k_{\perp}$.

But where does the inertial range start?

- Injection of energy is done by linear instabilities.
- At large scales, the growth rate of the most unstable modes (usually) satisfies $\gamma_{\boldsymbol{k}} \propto k_y$.
- The outer scale $\boldsymbol{k}^{\mathrm{o}}$ is the scale where

$$\gamma^{\mathrm{o}} \sim \tau_{\mathrm{nl}}^{\mathrm{o}\,-1}. \tag{14}$$

This is where the dominant injection of energy happens.

- Beyond the outer scale, nonlinearity dominates as $\tau_{\mathrm{nl}}^{-1} \propto k_{\perp}^{4/3} \gg \gamma_{\boldsymbol{k}} \sim k_{\perp}$.
- The dominant contribution to the heat flux Q_s comes from the outer scale:

$$Q_s \sim Q_s^{\mathrm{o}} \sim n_{0s} T_{0s} v_{\mathrm{th}s} k_y^{\mathrm{o}} \rho_s \overline{\varphi}^{\mathrm{o}\,2} \propto k_y^{\mathrm{o}} \overline{\varphi}^{\mathrm{o}\,2}. \tag{15}$$

But where does the inertial range start?

- Injection of energy is done by linear instabilities.
- At large scales, the growth rate of the most unstable modes (usually) satisfies $\gamma_{\boldsymbol{k}} \propto k_y$.
- The outer scale $\boldsymbol{k}^{\mathrm{o}}$ is the scale where

$$\gamma^{\mathrm{o}} \sim \tau_{\mathrm{nl}}^{\mathrm{o}\ -1}. \tag{14}$$

  This is where the dominant injection of energy happens.
- Beyond the outer scale, nonlinearity dominates as $\tau_{\mathrm{nl}}^{-1} \propto k_\perp^{4/3} \gg \gamma_{\boldsymbol{k}} \sim k_\perp$.
- The dominant contribution to the heat flux Q_s comes from the outer scale:

$$Q_s \sim Q_s^{\mathrm{o}} \sim n_{0s} T_{0s} v_{\mathrm{th}s} k_y^{\mathrm{o}} \rho_s \overline{\varphi}^{\mathrm{o}2} \propto k_y^{\mathrm{o}} \overline{\varphi}^{\mathrm{o}2}. \tag{15}$$

- To predict Q_s, we seek predictions for
  (i) the outer scale k_y^{o},
  (ii) the outer-scale amplitude $\overline{\varphi}^{\mathrm{o}}$.

Determining the outer scale

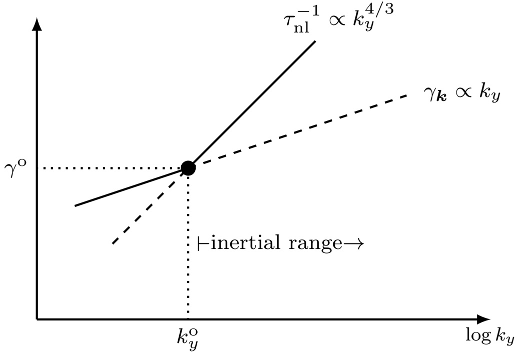

Parallel structure and critical balance

- We have two unknowns, k_y^{o} and $\overline{\varphi}^{\mathrm{o}}$, but only one equation, viz., $\gamma^{\mathrm{o}} \sim {\tau_{\mathrm{nl}}^{\mathrm{o}}}^{-1}$.

Parallel structure and critical balance

- We have two unknowns, k_y^{o} and $\overline{\varphi}^{\mathrm{o}}$, but only one equation, viz., $\gamma^{\mathrm{o}} \sim {\tau_{\mathrm{nl}}^{\mathrm{o}}}^{-1}$.
- Need one more constraint...

Parallel structure and critical balance

- We have two unknowns, k_y^{o} and $\overline{\varphi}^{\mathrm{o}}$, but only one equation, viz., $\gamma^{\mathrm{o}} \sim {\tau_{\mathrm{nl}}^{\mathrm{o}}}^{-1}$.
- Need one more constraint... Barnes et al. (2011) uses 'critical balance' $\gamma^{\mathrm{o}} \sim \omega_{\parallel}^{\mathrm{o}}$ with the parallel time scale $\omega_{\parallel} \sim k_{\parallel} v_{\mathrm{th}s}$ at the 'system scale' $k_{\parallel}^{\mathrm{o}} qR \sim 1$ to find

$$Q_s \sim n_{0s} T_{0s} v_{\mathrm{th}s} \left(\frac{\rho_s}{R}\right)^2 \left(\frac{R}{L_{T_s}}\right)^3 q. \tag{16}$$

Parallel structure and critical balance

- We have two unknowns, k_y^{o} and $\overline{\varphi}^{\mathrm{o}}$, but only one equation, viz., $\gamma^{\mathrm{o}} \sim {\tau_{\mathrm{nl}}^{\mathrm{o}}}^{-1}$.
- Need one more constraint... Barnes et al. (2011) uses 'critical balance' $\gamma^{\mathrm{o}} \sim \omega_{\parallel}^{\mathrm{o}}$ with the parallel time scale $\omega_{\parallel} \sim k_{\parallel} v_{\mathrm{th}s}$ at the 'system scale' $k_{\parallel}^{\mathrm{o}} qR \sim 1$ to find

$$Q_s \sim n_{0s} T_{0s} v_{\mathrm{th}s} \left(\frac{\rho_s}{R}\right)^2 \left(\frac{R}{L_{T_s}}\right)^3 q. \tag{16}$$

- Another interesting case is 'Grand critical balance' (Ghim et al., 2013; Nies et al., 2023): instead of $\mathcal{A}^{\mathrm{o}} \sim 1$, suppose that k_x^{o} is determined by

$$\omega_{ds,x}^{\mathrm{o}} \sim \gamma^{\mathrm{o}} \sim {\tau_{\mathrm{nl}}^{\mathrm{o}}}^{-1} \sim \omega_{\parallel}^{\mathrm{o}}. \tag{17}$$

Yields $\mathcal{A}^{\mathrm{o}} \sim R/L_{T_s}$ and

$$Q_s \sim n_{0s} T_{0s} v_{\mathrm{th}s} \left(\frac{\rho_s}{R}\right)^2 \frac{R}{L_{T_s}} q. \tag{18}$$

To what are we adding flow shear?

- The theory of flow-shear suppression will be agnostic to the way in which the outer scale is chosen in the absence of shear...

To what are we adding flow shear?

- The theory of flow-shear suppression will be agnostic to the way in which the outer scale is chosen in the absence of shear...
- ... as well as to the dynamics in the inertial range. **We focus on the transport-defining outer scale.**

To what are we adding flow shear?

- The theory of flow-shear suppression will be agnostic to the way in which the outer scale is chosen in the absence of shear...
- ... as well as to the dynamics in the inertial range. **We focus on the transport-defining outer scale.**
- Anticipating what turns out to be interesting, we consider streamer-dominated turbulence with $\mathcal{A}^{\mathrm{o}} < 1$.

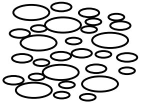

$\mathcal{A} < 1$

Outline

Adding flow shear

$$\left(\frac{\partial}{\partial t} + \boldsymbol{u}\cdot\frac{\partial}{\partial \boldsymbol{R}_s}\right)\left(h_s - \frac{q_s \left\langle \phi \right\rangle_{\boldsymbol{R}_s}}{T_{0s}} f_{0s}\right) + v_\parallel \boldsymbol{b}_0 \cdot \frac{\partial h_s}{\partial \boldsymbol{R}_s} + \boldsymbol{v}_{ds}\cdot\frac{\partial h_s}{\partial \boldsymbol{R}_s} + \boldsymbol{v}_E\cdot\frac{\partial}{\partial \boldsymbol{R}_s}\left(f_{0s} + h_s\right) = \sum_{s'} C_{ss'}, \tag{19}$$

Adding flow shear

$$\left(\frac{\partial}{\partial t} + \boldsymbol{u} \cdot \frac{\partial}{\partial \boldsymbol{R}_s}\right)\left(h_s - \frac{q_s \langle \phi \rangle_{\boldsymbol{R}_s}}{T_{0s}} f_{0s}\right) + v_\parallel \boldsymbol{b}_0 \cdot \frac{\partial h_s}{\partial \boldsymbol{R}_s} + \boldsymbol{v}_{ds} \cdot \frac{\partial h_s}{\partial \boldsymbol{R}_s} + \boldsymbol{v}_E \cdot \frac{\partial}{\partial \boldsymbol{R}_s}\left(f_{0s} + h_s\right) = \sum_{s'} C_{ss'}, \tag{19}$$

- In axisymmetric devices, $\boldsymbol{u}$ is toroidal.

Adding flow shear

$$\left(\frac{\partial}{\partial t} + \boldsymbol{u} \cdot \frac{\partial}{\partial \boldsymbol{R}_s}\right)\left(h_s - \frac{q_s \langle\phi\rangle_{\boldsymbol{R}_s}}{T_{0s}} f_{0s}\right) + v_\parallel \boldsymbol{b}_0 \cdot \frac{\partial h_s}{\partial \boldsymbol{R}_s} + \boldsymbol{v}_{ds} \cdot \frac{\partial h_s}{\partial \boldsymbol{R}_s} + \boldsymbol{v}_E \cdot \frac{\partial}{\partial \boldsymbol{R}_s}\left(f_{0s} + h_s\right) = \sum_{s'} C_{ss'}, \tag{19}$$

- In axisymmetric devices, $\boldsymbol{u}$ is toroidal.
- Mean flow shear can suppress instabilities...

Adding flow shear

$$\left(\frac{\partial}{\partial t} + \boldsymbol{u} \cdot \frac{\partial}{\partial \boldsymbol{R}_s}\right)\left(h_s - \frac{q_s \langle \phi \rangle_{\boldsymbol{R}_s}}{T_{0s}} f_{0s}\right) + v_{\parallel} \boldsymbol{b}_0 \cdot \frac{\partial h_s}{\partial \boldsymbol{R}_s} + \boldsymbol{v}_{ds} \cdot \frac{\partial h_s}{\partial \boldsymbol{R}_s} + \boldsymbol{v}_E \cdot \frac{\partial}{\partial \boldsymbol{R}_s}\left(f_{0s} + h_s\right) = \sum_{s'} C_{ss'}, \tag{19}$$

- In axisymmetric devices, $\boldsymbol{u}$ is toroidal.
- Mean flow shear can suppress instabilities...
- but it can also drive them: PVG!

Adding flow shear

$$\left(\frac{\partial}{\partial t} + \boldsymbol{u} \cdot \frac{\partial}{\partial \boldsymbol{R}_s}\right)\left(h_s - \frac{q_s \left\langle \phi \right\rangle_{\boldsymbol{R}_s}}{T_{0s}} f_{0s}\right) + v_\parallel \boldsymbol{b}_0 \cdot \frac{\partial h_s}{\partial \boldsymbol{R}_s} + \boldsymbol{v}_{ds} \cdot \frac{\partial h_s}{\partial \boldsymbol{R}_s} + \boldsymbol{v}_E \cdot \frac{\partial}{\partial \boldsymbol{R}_s}\left(f_{0s} + h_s\right) = \sum_{s'} C_{ss'}, \tag{19}$$

- In axisymmetric devices, $\boldsymbol{u}$ is toroidal.
- Mean flow shear can suppress instabilities...
- but it can also drive them: PVG!

For the remainder of this talk, we will take $\boldsymbol{u}$ to be perpendicular to the magnetic field!

Adding flow shear

- Include sheared mean flow of the form

$$\boldsymbol{u} = \gamma_E x \boldsymbol{y}. \tag{20}$$

Adding flow shear

- Include sheared mean flow of the form

$$\boldsymbol{u} = \gamma_E x \boldsymbol{y}. \tag{20}$$

- GK no longer homogeneous in x!

Adding flow shear

- Include sheared mean flow of the form

$$\boldsymbol{u} = \gamma_E x \boldsymbol{y}. \tag{20}$$

- GK no longer homogeneous in x!
- Instructive to think about the shearing-frame transformation in a slab:

Adding flow shear

- Include sheared mean flow of the form

$$\boldsymbol{u} = \gamma_E x \boldsymbol{y}. \tag{20}$$

- GK no longer homogeneous in x!
- Instructive to think about the shearing-frame transformation in a slab:

$$t' = t,\ x' = x,\ y' = y - x\gamma_E t,\ z' = z, \tag{21}$$

Adding flow shear

- Include sheared mean flow of the form

$$\boldsymbol{u} = \gamma_E x \boldsymbol{y}. \tag{20}$$

- GK no longer homogeneous in x!
- Instructive to think about the shearing-frame transformation in a slab:

$$t' = t,\ x' = x,\ y' = y - x\gamma_E t,\ z' = z, \tag{21}$$

- Eliminates the inhomogeneous advection term $\boldsymbol{u} \cdot \boldsymbol{\nabla}$!

Adding flow shear

- Include sheared mean flow of the form

$$\boldsymbol{u} = \gamma_E x \boldsymbol{y}. \tag{20}$$

- GK no longer homogeneous in x!
- Instructive to think about the shearing-frame transformation in a slab:

$$t' = t, \;\; x' = x, \;\; y' = y - x\gamma_E t, \;\; z' = z, \tag{21}$$

- Eliminates the inhomogeneous advection term $\boldsymbol{u} \cdot \boldsymbol{\nabla}$!
- ... but at the cost of introducing an inhomogeneity in time via the ∂_x derivatives.

Adding flow shear

- Include sheared mean flow of the form

$$\boldsymbol{u} = \gamma_E x \boldsymbol{y}. \tag{20}$$

- GK no longer homogeneous in x!
- Instructive to think about the shearing-frame transformation in a slab:

$$t' = t,\ x' = x,\ y' = y - x\gamma_E t,\ z' = z, \tag{21}$$

- Eliminates the inhomogeneous advection term $\boldsymbol{u} \cdot \boldsymbol{\nabla}$!
- ... but at the cost of introducing an inhomogeneity in time via the ∂_x derivatives.
- The 'lab-frame' radial wavenumber 'drifts':

$$k_x = k_x' - k_y' \gamma_E t'. \tag{22}$$

Eddy 'tilting'

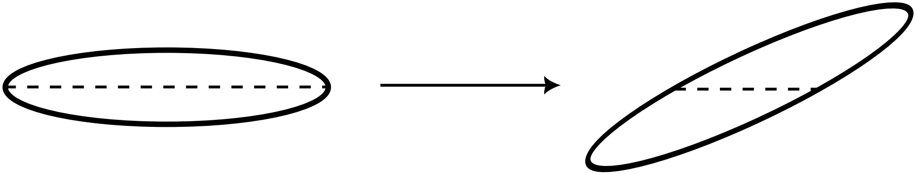

Eddy 'tilting'

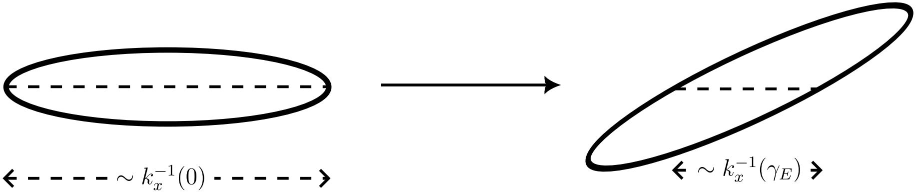

Eddy 'tilting'

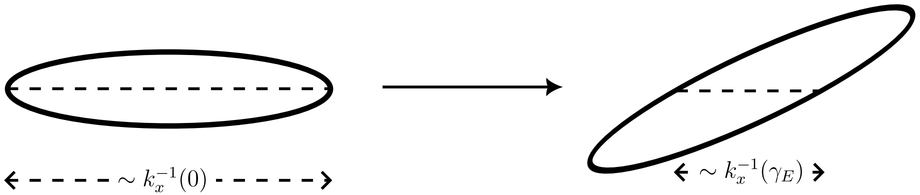

- In what follows, we will use $f(\gamma_E)$ to denote dependence on γ_E.

Eddy 'tilting'

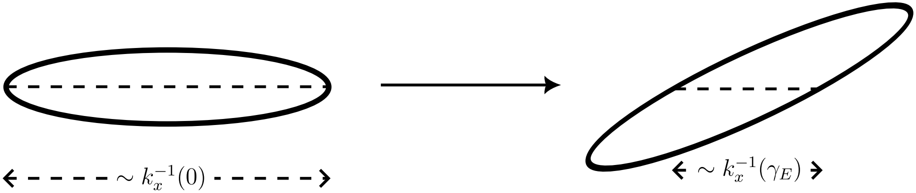

- In what follows, we will use $f(\gamma_E)$ to denote dependence on γ_E.
- E.g., $k_y^{\mathrm{o}}(0)$ and $\gamma^{\mathrm{o}}(0)$ refer to the outer-scale wavenumber and injection rate in the absence of flow shear.

Adding flow shear

Adding flow shear

- Consider a system that, in the absence of flow shear, saturates with an outer scale $k_y^{\mathrm{o}}(0)$ and injection rate $\gamma^{\mathrm{o}}(0)$.

Adding flow shear

- Consider a system that, in the absence of flow shear, saturates with an outer scale $k_y^{\mathrm{o}}(0)$ and injection rate $\gamma^{\mathrm{o}}(0)$.
- At the outer scale, $\tau_{\mathrm{nl}}^{\mathrm{o}}(0)^{-1} \sim \gamma^{\mathrm{o}}(0)$.

Adding flow shear

- Consider a system that, in the absence of flow shear, saturates with an outer scale $k_y^{\mathrm{o}}(0)$ and injection rate $\gamma^{\mathrm{o}}(0)$.
- At the outer scale, $\tau_{\mathrm{nl}}^{\mathrm{o}}(0)^{-1} \sim \gamma^{\mathrm{o}}(0)$.
- In the presence of flow shear, we distinguish two regimes:
  (i) **weakly sheared regime** with $\gamma_E < \gamma^{\mathrm{o}}(0)$,
  (ii) **strongly sheared regime** with $\gamma_E > \gamma^{\mathrm{o}}(0)$.

Adding flow shear

- Consider a system that, in the absence of flow shear, saturates with an outer scale $k_y^{\mathrm{o}}(0)$ and injection rate $\gamma^{\mathrm{o}}(0)$.
- At the outer scale, $\tau_{\mathrm{nl}}^{\mathrm{o}}(0)^{-1} \sim \gamma^{\mathrm{o}}(0)$.
- In the presence of flow shear, we distinguish two regimes:
  (i) **weakly sheared regime** with $\gamma_E < \gamma^{\mathrm{o}}(0)$,
  (ii) **strongly sheared regime** with $\gamma_E > \gamma^{\mathrm{o}}(0)$.
- Motivated by the quench rule (Waltz et al., 1998).

Adding flow shear

- Consider a system that, in the absence of flow shear, saturates with an outer scale $k_y^{\rm o}(0)$ and injection rate $\gamma^{\rm o}(0)$.
- At the outer scale, $\tau_{\rm nl}^{\rm o}(0)^{-1} \sim \gamma^{\rm o}(0)$.
- In the presence of flow shear, we distinguish two regimes:
  (i) **weakly sheared regime** with $\gamma_E < \gamma^{\rm o}(0)$,
  (ii) **strongly sheared regime** with $\gamma_E > \gamma^{\rm o}(0)$.
- Motivated by the quench rule (Waltz et al., 1998).
- Hypotheses:
  (i) In the weakly sheared regime, $k_y^{\rm o}$ and $\gamma^{\rm o}$ are independent of γ_E, viz., $k_y^{\rm o} \approx k_y^{\rm o}(0)$, $\gamma^{\rm o} \approx \gamma^{\rm o}(0)$.

Adding flow shear

- Consider a system that, in the absence of flow shear, saturates with an outer scale $k_y^{\mathrm{o}}(0)$ and injection rate $\gamma^{\mathrm{o}}(0)$.
- At the outer scale, $\tau_{\mathrm{nl}}^{\mathrm{o}}(0)^{-1} \sim \gamma^{\mathrm{o}}(0)$.
- In the presence of flow shear, we distinguish two regimes:
  (i) **weakly sheared regime** with $\gamma_E < \gamma^{\mathrm{o}}(0)$,
  (ii) **strongly sheared regime** with $\gamma_E > \gamma^{\mathrm{o}}(0)$.
- Motivated by the quench rule (Waltz et al., 1998).
- Hypotheses:
  (i) In the weakly sheared regime, k_y^{o} and γ^{o} are independent of γ_E, viz., $k_y^{\mathrm{o}} \approx k_y^{\mathrm{o}}(0)$, $\gamma^{\mathrm{o}} \approx \gamma^{\mathrm{o}}(0)$.
  (ii) In the strongly sheared regime, the outer scale is governed by $\gamma^{\mathrm{o}}(\gamma_E) \sim \tau_{\mathrm{nl}}^{\mathrm{o}}(\gamma_E)^{-1} \sim \gamma_E$.

Weakly sheared regime

- For $\gamma_E < \gamma^{\text{o}}(0)$, we assume that

$$\tau_{\text{nl}}^{\text{o}}(\gamma_E)^{-1} \sim \gamma^{\text{o}}(\gamma_E) \sim \gamma^{\text{o}}(0) \sim \tau_{\text{nl}}^{\text{o}}(0)^{-1}. \tag{23}$$

Weakly sheared regime

- For $\gamma_E < \gamma^{\mathrm{o}}(0)$, we assume that

$$\tau_{\mathrm{nl}}^{\mathrm{o}}(\gamma_E)^{-1} \sim \gamma^{\mathrm{o}}(\gamma_E) \sim \gamma^{\mathrm{o}}(0) \sim \tau_{\mathrm{nl}}^{\mathrm{o}}(0)^{-1}. \tag{23}$$

- Assuming that $\gamma_{\boldsymbol{k}} \propto k_y$ is (approximately) independent of k_x, we find that $k_y^{\mathrm{o}}(\gamma_E) \approx k_y^{\mathrm{o}}(0)$.

Weakly sheared regime

- For $\gamma_E < \gamma^{\rm o}(0)$, we assume that

$$\tau^{\rm o}_{\rm nl}(\gamma_E)^{-1} \sim \gamma^{\rm o}(\gamma_E) \sim \gamma^{\rm o}(0) \sim \tau^{\rm o}_{\rm nl}(0)^{-1}. \tag{23}$$

- Assuming that $\gamma_{\boldsymbol{k}} \propto k_y$ is (approximately) independent of k_x, we find that $k_y^{\rm o}(\gamma_E) \approx k_y^{\rm o}(0)$.
- Cannot say the same about $k_x^{\rm o}(\gamma_E)$!

Weakly sheared regime

- For $\gamma_E < \gamma^{\mathrm{o}}(0)$, we assume that

$$\tau_{\mathrm{nl}}^{\mathrm{o}}(\gamma_E)^{-1} \sim \gamma^{\mathrm{o}}(\gamma_E) \sim \gamma^{\mathrm{o}}(0) \sim \tau_{\mathrm{nl}}^{\mathrm{o}}(0)^{-1}. \tag{23}$$

- Assuming that $\gamma_{\boldsymbol{k}} \propto k_y$ is (approximately) independent of k_x, we find that $k_y^{\mathrm{o}}(\gamma_E) \approx k_y^{\mathrm{o}}(0)$.
- Cannot say the same about $k_x^{\mathrm{o}}(\gamma_E)$!
- The eddy 'tilting' $k_x = k_x' - k_y'\gamma_E t'$ suggests that

$$k_x^{\mathrm{o}}(\gamma_E) \sim k_x^{\mathrm{o}}(0) + k_y^{\mathrm{o}}(0)\gamma_E \tau_{\mathrm{nl}}^{\mathrm{o}}(0). \tag{24}$$

Weakly sheared regime

- For $\gamma_E < \gamma^{\mathrm{o}}(0)$, we assume that

$$\tau_{\mathrm{nl}}^{\mathrm{o}}(\gamma_E)^{-1} \sim \gamma^{\mathrm{o}}(\gamma_E) \sim \gamma^{\mathrm{o}}(0) \sim \tau_{\mathrm{nl}}^{\mathrm{o}}(0)^{-1}. \tag{23}$$

- Assuming that $\gamma_{\boldsymbol{k}} \propto k_y$ is (approximately) independent of k_x, we find that $k_y^{\mathrm{o}}(\gamma_E) \approx k_y^{\mathrm{o}}(0)$.
- Cannot say the same about $k_x^{\mathrm{o}}(\gamma_E)$!
- The eddy 'tilting' $k_x = k_x' - k_y'\gamma_E t'$ suggests that

$$k_x^{\mathrm{o}}(\gamma_E) \sim k_x^{\mathrm{o}}(0) + k_y^{\mathrm{o}}(0)\gamma_E\tau_{\mathrm{nl}}^{\mathrm{o}}(0). \tag{24}$$

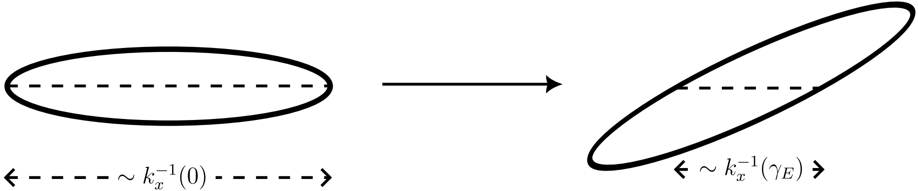

Weakly sheared regime

- For $\gamma_E < \gamma^{\text{o}}(0)$, we assume that

$$\tau_{\text{nl}}^{\text{o}}(\gamma_E)^{-1} \sim \gamma^{\text{o}}(\gamma_E) \sim \gamma^{\text{o}}(0) \sim \tau_{\text{nl}}^{\text{o}}(0)^{-1}. \tag{23}$$

- Assuming that $\gamma_{\boldsymbol{k}} \propto k_y$ is (approximately) independent of k_x, we find that $k_y^{\text{o}}(\gamma_E) \approx k_y^{\text{o}}(0)$.
- Cannot say the same about $k_x^{\text{o}}(\gamma_E)$!
- The eddy 'tilting' $k_x = k_x' - k_y'\gamma_E t'$ suggests that

$$k_x^{\text{o}}(\gamma_E) \sim k_x^{\text{o}}(0) + k_y^{\text{o}}(0)\gamma_E\tau_{\text{nl}}^{\text{o}}(0). \tag{24}$$

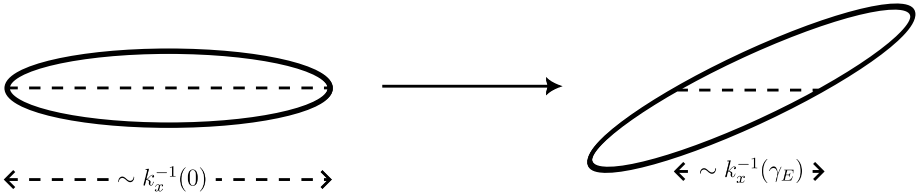

The eddies tilt, but keep the same poloidal scale.

Weakly sheared regime

- Assuming $k_x^{\mathrm{o}}(\gamma_E) \sim k_x^{\mathrm{o}}(0) + k_y^{\mathrm{o}}(0)\tau_{\mathrm{nl}}^{\mathrm{o}}(0)\gamma_E$, we get

$$\Longrightarrow \frac{k_x^{\mathrm{o}}(\gamma_E)}{k_x^{\mathrm{o}}(0)} \sim \frac{\mathcal{A}^{\mathrm{o}}(\gamma_E)}{\mathcal{A}^{\mathrm{o}}(0)} \sim 1 + \frac{\gamma_E}{\gamma_{\mathrm{c}}}, \tag{25}$$

  where we have defined the **critical shearing rate**

$$\gamma_{\mathrm{c}} \equiv \mathcal{A}^{\mathrm{o}}(0)\gamma^{\mathrm{o}}(0) < \gamma^{\mathrm{o}}(0). \tag{26}$$

Weakly sheared regime

- Assuming $k_x^{\mathrm{o}}(\gamma_E) \sim k_x^{\mathrm{o}}(0) + k_y^{\mathrm{o}}(0)\tau_{\mathrm{nl}}^{\mathrm{o}}(0)\gamma_E$, we get

$$\Longrightarrow \frac{k_x^{\mathrm{o}}(\gamma_E)}{k_x^{\mathrm{o}}(0)} \sim \frac{\mathcal{A}^{\mathrm{o}}(\gamma_E)}{\mathcal{A}^{\mathrm{o}}(0)} \sim 1 + \frac{\gamma_E}{\gamma_{\mathrm{c}}}, \tag{25}$$

where we have defined the **critical shearing rate**

$$\gamma_{\mathrm{c}} \equiv \mathcal{A}^{\mathrm{o}}(0)\gamma^{\mathrm{o}}(0) < \gamma^{\mathrm{o}}(0). \tag{26}$$

- Plugging (25) into

$$\tau_{\mathrm{nl}}^{-1} \sim \mathcal{A}\Omega_s \rho_s^2 k_y^2 \overline{\varphi}, \tag{27}$$

we get

$$\frac{\overline{\varphi}^{\mathrm{o}}(\gamma_E)}{\overline{\varphi}^{\mathrm{o}}(0)} \sim \frac{\mathcal{A}^{\mathrm{o}}(0)}{\mathcal{A}^{\mathrm{o}}(\gamma_E)} \sim \frac{1}{1 + \gamma_E/\gamma_{\mathrm{c}}} \tag{28}$$

Weakly sheared regime

- Assuming $k_x^{\mathrm{o}}(\gamma_E) \sim k_x^{\mathrm{o}}(0) + k_y^{\mathrm{o}}(0)\tau_{\mathrm{nl}}^{\mathrm{o}}(0)\gamma_E$, we get

$$\Longrightarrow \frac{k_x^{\mathrm{o}}(\gamma_E)}{k_x^{\mathrm{o}}(0)} \sim \frac{\mathcal{A}^{\mathrm{o}}(\gamma_E)}{\mathcal{A}^{\mathrm{o}}(0)} \sim 1 + \frac{\gamma_E}{\gamma_{\mathrm{c}}}, \tag{25}$$

where we have defined the **critical shearing rate**

$$\gamma_{\mathrm{c}} \equiv \mathcal{A}^{\mathrm{o}}(0)\gamma^{\mathrm{o}}(0) < \gamma^{\mathrm{o}}(0). \tag{26}$$

- Plugging (25) into

$$\tau_{\mathrm{nl}}^{-1} \sim \mathcal{A}\Omega_s \rho_s^2 k_y^2 \overline{\varphi}, \tag{27}$$

we get

$$\frac{\overline{\varphi}^{\mathrm{o}}(\gamma_E)}{\overline{\varphi}^{\mathrm{o}}(0)} \sim \frac{\mathcal{A}^{\mathrm{o}}(0)}{\mathcal{A}^{\mathrm{o}}(\gamma_E)} \sim \frac{1}{1 + \gamma_E/\gamma_{\mathrm{c}}} \tag{28}$$

- Using $Q \sim Q^{\mathrm{o}} \propto k_y^{\mathrm{o}} \overline{\varphi}^{\mathrm{o}\,2}$, this leads to the heat-flux scaling

$$\frac{Q(\gamma_E)}{Q(0)} \sim \left[\frac{\mathcal{A}^{\mathrm{o}}(0)}{\mathcal{A}^{\mathrm{o}}(\gamma_E)}\right]^2 \sim \frac{1}{(1 + \gamma_E/\gamma_{\mathrm{c}})^2}. \tag{29}$$

Weakly sheared regime

Weakly sheared regime

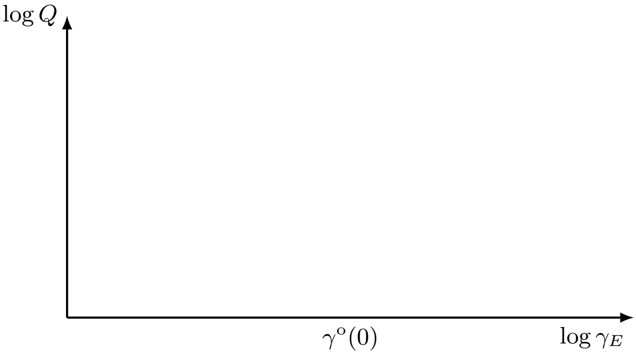

Weakly sheared regime

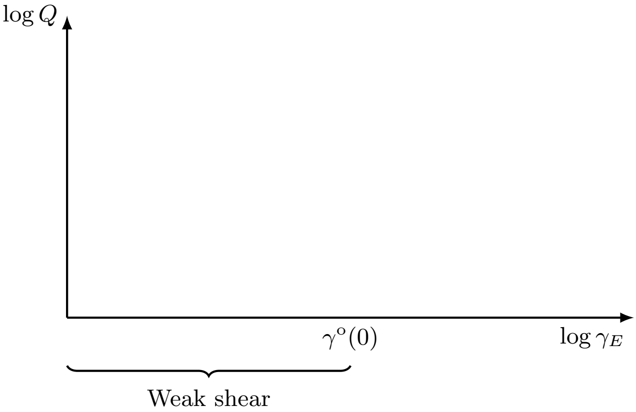

Weakly sheared regime

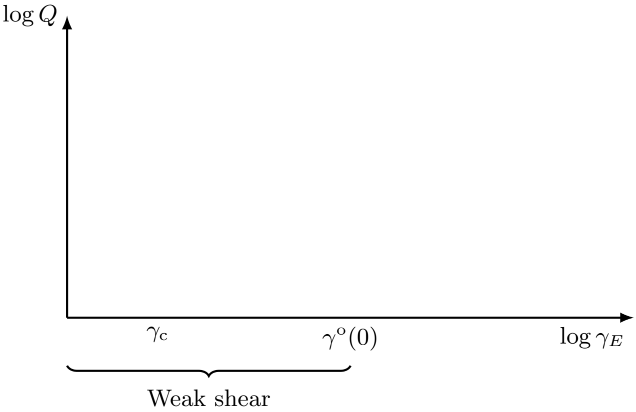

Weakly sheared regime

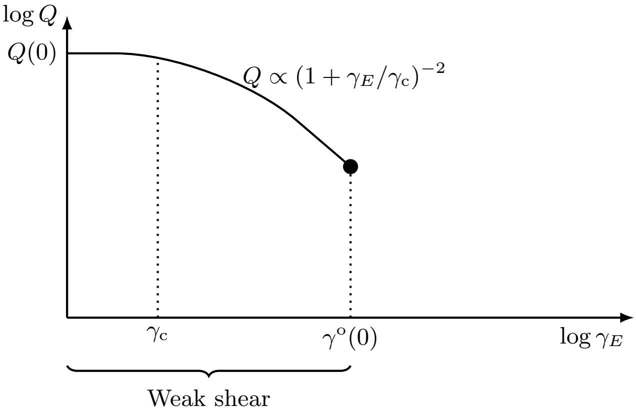

Weakly sheared regime

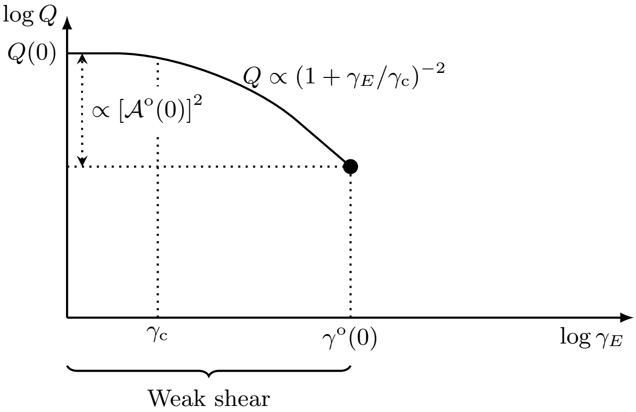

Weakly sheared regime

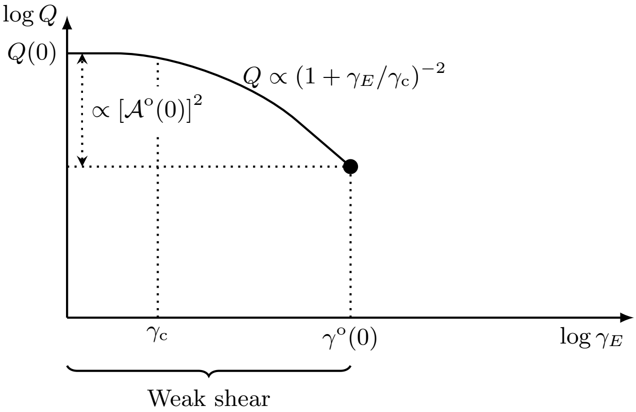

- Nothing much happens if $\mathcal{A}^{\circ}(0) \sim 1$.

Weakly sheared regime

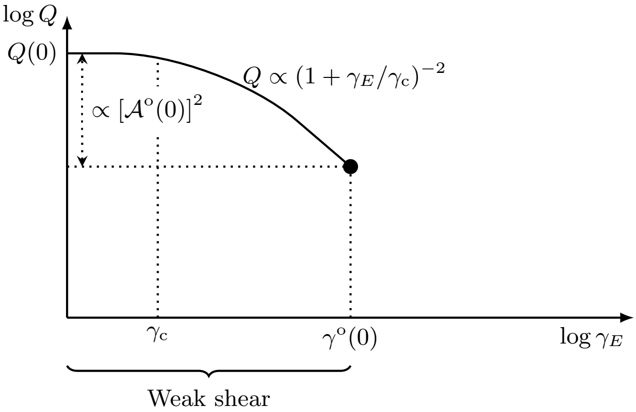

- Nothing much happens if $\mathcal{A}^{\circ}(0) \sim 1$.
- **Strong suppression if $\mathcal{A}^{\circ}(0) \ll 1$!**

Strongly sheared regime

- For $\gamma_E > \gamma^{\mathrm{o}}(0)$, we conjecture an outer-scale balance of the form

$$\tau_{\mathrm{nl}}^{\mathrm{o}}(\gamma_E)^{-1} \sim \gamma^{\mathrm{o}}(\gamma_E) \sim \gamma_E.$$

Strongly sheared regime

- For $\gamma_E > \gamma^{\rm o}(0)$, we conjecture an outer-scale balance of the form

$$\tau_{\rm nl}^{\rm o}(\gamma_E)^{-1} \sim \gamma^{\rm o}(\gamma_E) \sim \gamma_E.$$

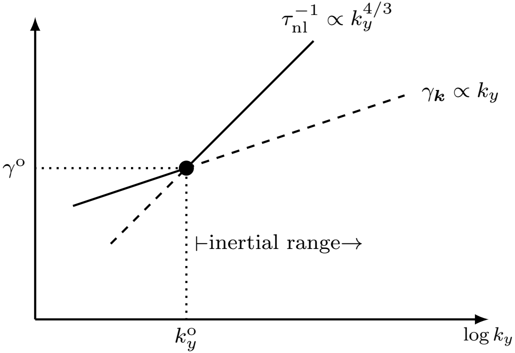

Strongly sheared regime

- For $\gamma_E > \gamma^{\rm o}(0)$, we conjecture an outer-scale balance of the form

$$\tau_{\rm nl}^{\rm o}(\gamma_E)^{-1} \sim \gamma^{\rm o}(\gamma_E) \sim \gamma_E.$$

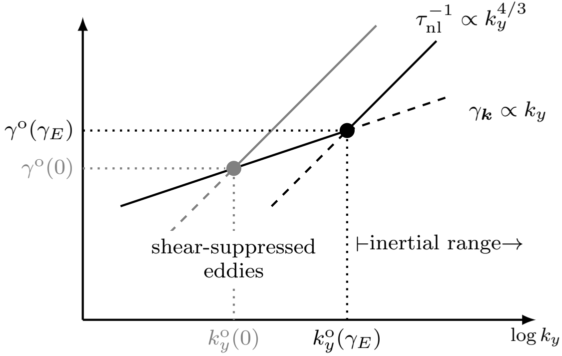

Strongly sheared regime

- For $\gamma_E > \gamma^{\mathrm{o}}(0)$, we conjecture an outer-scale balance of the form

$$\tau_{\mathrm{nl}}^{\mathrm{o}}(\gamma_E)^{-1} \sim \gamma^{\mathrm{o}}(\gamma_E) \sim \gamma_E.$$

Strongly sheared regime

- For $\gamma_E > \gamma^{\mathrm{o}}(0)$, we conjecture an outer-scale balance of the form
$$\tau_{\mathrm{nl}}^{\mathrm{o}}(\gamma_E)^{-1} \sim \gamma^{\mathrm{o}}(\gamma_E) \sim \gamma_E.$$

- Assuming $\gamma_{\boldsymbol{k}} \propto k_y$, we find $k_y^{\mathrm{o}}(\gamma_E) \propto \gamma_E$.

Strongly sheared regime

- For $\gamma_E > \gamma^{\mathrm{o}}(0)$, we conjecture an outer-scale balance of the form

$$\tau_{\mathrm{nl}}^{\mathrm{o}}(\gamma_E)^{-1} \sim \gamma^{\mathrm{o}}(\gamma_E) \sim \gamma_E.$$

- Assuming $\gamma_{\boldsymbol{k}} \propto k_y$, we find $k_y^{\mathrm{o}}(\gamma_E) \propto \gamma_E$.
- The eddy 'tilting' $k_x = k_x' - k_y' \gamma_E t'$ and balance $\tau_{\mathrm{nl}}^{\mathrm{o}}(\gamma_E)^{-1} \sim \gamma_E$ suggest that

$$k_x^{\mathrm{o}}(\gamma_E) \sim k_y^{\mathrm{o}}(\gamma_E)\gamma_E \tau_{\mathrm{nl}}^{\mathrm{o}}(\gamma_E) \sim k_y^{\mathrm{o}}(\gamma_E). \quad (30)$$

  and so $\mathcal{A}^{\mathrm{o}}(\gamma_E) \sim 1$

Strongly sheared regime

- For $\gamma_E > \gamma^{\mathrm{o}}(0)$, we conjecture an outer-scale balance of the form
$$\tau_{\mathrm{nl}}^{\mathrm{o}}(\gamma_E)^{-1} \sim \gamma^{\mathrm{o}}(\gamma_E) \sim \gamma_E.$$

- Assuming $\gamma_{\boldsymbol{k}} \propto k_y$, we find $k_y^{\mathrm{o}}(\gamma_E) \propto \gamma_E$.
- The eddy 'tilting' $k_x = k_x' - k_y'\gamma_E t'$ and balance $\tau_{\mathrm{nl}}^{\mathrm{o}}(\gamma_E)^{-1} \sim \gamma_E$ suggest that
$$k_x^{\mathrm{o}}(\gamma_E) \sim k_y^{\mathrm{o}}(\gamma_E)\gamma_E\tau_{\mathrm{nl}}^{\mathrm{o}}(\gamma_E) \sim k_y^{\mathrm{o}}(\gamma_E). \tag{30}$$

and so $\mathcal{A}^{\mathrm{o}}(\gamma_E) \sim 1$

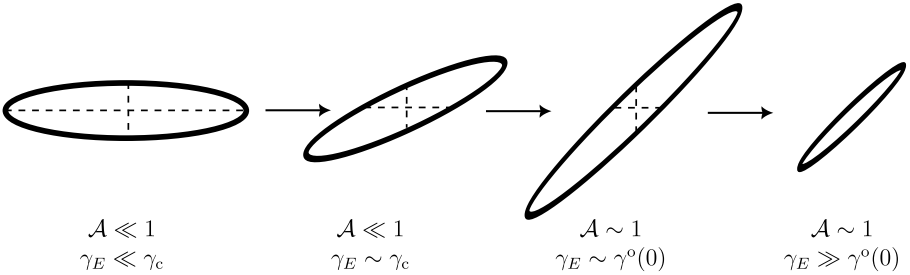

Strongly sheared regime

- Using $k_y^{\mathrm{o}}(\gamma_E) \sim k_x^{\mathrm{o}}(\gamma_E) \propto \gamma_E$ and $\tau_{\mathrm{nl}}^{\mathrm{o}}(\gamma_E)^{-1} \sim \gamma_E$, we get

$$\overline{\varphi}^{\mathrm{o}}(\gamma_E) \propto \frac{\tau_{\mathrm{nl}}^{\mathrm{o}}(\gamma_E)^{-1}}{\mathcal{A}^{\mathrm{o}}(\gamma_E) k_y^{\mathrm{o}}(\gamma_E)^2} \propto \gamma_E^{-1}, \tag{31}$$

Strongly sheared regime

- Using $k_y^{\mathrm{o}}(\gamma_E) \sim k_x^{\mathrm{o}}(\gamma_E) \propto \gamma_E$ and $\tau_{\mathrm{nl}}^{\mathrm{o}}(\gamma_E)^{-1} \sim \gamma_E$, we get

$$\overline{\varphi}^{\mathrm{o}}(\gamma_E) \propto \frac{\tau_{\mathrm{nl}}^{\mathrm{o}}(\gamma_E)^{-1}}{\mathcal{A}^{\mathrm{o}}(\gamma_E) k_y^{\mathrm{o}}(\gamma_E)^2} \propto \gamma_E^{-1}, \tag{31}$$

which, combined with $k_y^{\mathrm{o}}(\gamma_E) \propto \gamma_E$ yields

$$Q(\gamma_E) \sim k_y^{\mathrm{o}}(\gamma_E) \overline{\varphi}^{\mathrm{o}}(\gamma_E)^2 \propto \gamma_E^{-1}. \tag{32}$$

Strongly sheared regime

- Using $k_y^{\mathrm{o}}(\gamma_E) \sim k_x^{\mathrm{o}}(\gamma_E) \propto \gamma_E$ and $\tau_{\mathrm{nl}}^{\mathrm{o}}(\gamma_E)^{-1} \sim \gamma_E$, we get

$$\overline{\varphi}^{\mathrm{o}}(\gamma_E) \propto \frac{\tau_{\mathrm{nl}}^{\mathrm{o}}(\gamma_E)^{-1}}{\mathcal{A}^{\mathrm{o}}(\gamma_E) k_y^{\mathrm{o}}(\gamma_E)^2} \propto \gamma_E^{-1}, \tag{31}$$

which, combined with $k_y^{\mathrm{o}}(\gamma_E) \propto \gamma_E$ yields

$$Q(\gamma_E) \sim k_y^{\mathrm{o}}(\gamma_E) \overline{\varphi}^{\mathrm{o}}(\gamma_E)^2 \propto \gamma_E^{-1}. \tag{32}$$

- The balance $\gamma^{\mathrm{o}}(\gamma_E) \sim \gamma_E$ holds only for γ_E up to the largest growth rate $\gamma_{\max}$.

Strongly sheared regime

- Using $k_y^{\mathrm{o}}(\gamma_E) \sim k_x^{\mathrm{o}}(\gamma_E) \propto \gamma_E$ and $\tau_{\mathrm{nl}}^{\mathrm{o}}(\gamma_E)^{-1} \sim \gamma_E$, we get

$$\overline{\varphi}^{\mathrm{o}}(\gamma_E) \propto \frac{\tau_{\mathrm{nl}}^{\mathrm{o}}(\gamma_E)^{-1}}{\mathcal{A}^{\mathrm{o}}(\gamma_E) k_y^{\mathrm{o}}(\gamma_E)^2} \propto \gamma_E^{-1}, \tag{31}$$

  which, combined with $k_y^{\mathrm{o}}(\gamma_E) \propto \gamma_E$ yields

$$Q(\gamma_E) \sim k_y^{\mathrm{o}}(\gamma_E) \overline{\varphi}^{\mathrm{o}}(\gamma_E)^2 \propto \gamma_E^{-1}. \tag{32}$$

- The balance $\gamma^{\mathrm{o}}(\gamma_E) \sim \gamma_E$ holds only for γ_E up to the largest growth rate $\gamma_{\max}$.
- There lies the marginal regime...

Strongly sheared regime

- Using $k_y^{\mathrm{o}}(\gamma_E) \sim k_x^{\mathrm{o}}(\gamma_E) \propto \gamma_E$ and $\tau_{\mathrm{nl}}^{\mathrm{o}}(\gamma_E)^{-1} \sim \gamma_E$, we get

$$\overline{\varphi}^{\mathrm{o}}(\gamma_E) \propto \frac{\tau_{\mathrm{nl}}^{\mathrm{o}}(\gamma_E)^{-1}}{\mathcal{A}^{\mathrm{o}}(\gamma_E) k_y^{\mathrm{o}}(\gamma_E)^2} \propto \gamma_E^{-1}, \tag{31}$$

which, combined with $k_y^{\mathrm{o}}(\gamma_E) \propto \gamma_E$ yields

$$Q(\gamma_E) \sim k_y^{\mathrm{o}}(\gamma_E) \overline{\varphi}^{\mathrm{o}}(\gamma_E)^2 \propto \gamma_E^{-1}. \tag{32}$$

- The balance $\gamma^{\mathrm{o}}(\gamma_E) \sim \gamma_E$ holds only for γ_E up to the largest growth rate γ_{max}.
- There lies the marginal regime...bistability, coherent structures... beyond this talk!

Combining it all...

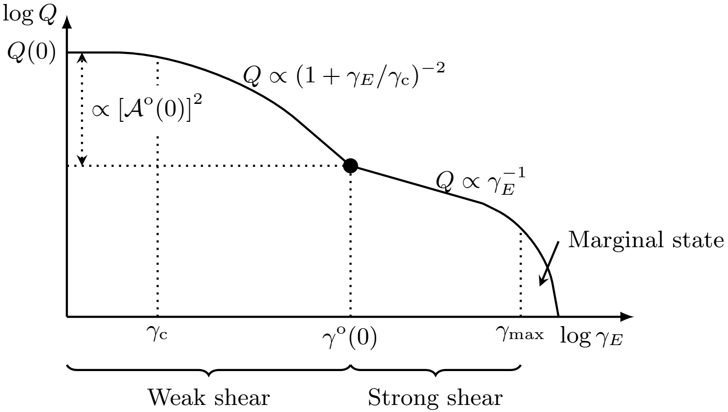

Outline

Numerical results

- Two different models:

Numerical results

- Two different models:
  (i) a slab model of fluid electron-scale turbulence.

Numerical results

- Two different models:
  (i) a slab model of fluid electron-scale turbulence.
  (ii) ion-scale GK with Cyclone-base-case geometry.

Fluid slab ETG model

We performed numerical simulations of the following collisional ETG model (first studied by Adkins et al., 2023)

$$\frac{\mathrm{d}}{\mathrm{d}t}\frac{\delta n_e}{n_{0e}} + \frac{\partial u_{\parallel e}}{\partial z} = 0, \tag{33}$$

$$\frac{\mathrm{d}}{\mathrm{d}t}\frac{\delta T_e}{T_{0e}} - \frac{c_3 v_{\mathrm{the}}^2}{3\nu_{ei}}\frac{\partial^2}{\partial z^2}\frac{\delta T_e}{T_{0e}} + \frac{2}{3}\left(1+\frac{c_2}{c_1}\right)\frac{\partial u_{\parallel e}}{\partial z} = -\frac{\rho_e v_{\mathrm{the}}}{2L_T}\frac{\partial \varphi}{\partial y}, \tag{34}$$

where $\varphi = e\phi/T_{0e}$,

$$\frac{\nu_{ei}}{c_1}\frac{u_{\parallel e}}{v_{\mathrm{the}}} = -\frac{v_{\mathrm{the}}}{2}\frac{\partial}{\partial z}\left[\frac{\delta n_e}{n_{0e}} - \varphi + \left(1+\frac{c_2}{c_1}\right)\frac{\delta T_e}{T_{0e}}\right], \tag{35}$$

and

$$\frac{\mathrm{d}}{\mathrm{d}t} = \frac{\partial}{\partial t} + \gamma_E x\frac{\partial}{\partial y} + \frac{\rho_e v_{\mathrm{the}}}{2}\left(\boldsymbol{z}\times\boldsymbol{\nabla}\varphi\right)\cdot\boldsymbol{\nabla} + \nu\nabla_\perp^4. \tag{36}$$

Fluid slab ETG model

We performed numerical simulations of the following collisional ETG model (first studied by Adkins et al., 2023)

$$\frac{\mathrm{d}}{\mathrm{d}t}\frac{\delta n_e}{n_{0e}} + \frac{\partial u_{\parallel e}}{\partial z} = 0, \tag{33}$$

$$\frac{\mathrm{d}}{\mathrm{d}t}\frac{\delta T_e}{T_{0e}} - \frac{c_3 v_{\mathrm{the}}^2}{3\nu_{ei}}\frac{\partial^2}{\partial z^2}\frac{\delta T_e}{T_{0e}} + \frac{2}{3}\left(1+\frac{c_2}{c_1}\right)\frac{\partial u_{\parallel e}}{\partial z} = -\frac{\rho_e v_{\mathrm{the}}}{2L_T}\frac{\partial \varphi}{\partial y}, \tag{34}$$

where $\varphi = e\phi/T_{0e}$,

$$\frac{\nu_{ei}}{c_1}\frac{u_{\parallel e}}{v_{\mathrm{the}}} = -\frac{v_{\mathrm{the}}}{2}\frac{\partial}{\partial z}\left[\frac{\delta n_e}{n_{0e}} - \varphi + \left(1+\frac{c_2}{c_1}\right)\frac{\delta T_e}{T_{0e}}\right], \tag{35}$$

and

$$\frac{\mathrm{d}}{\mathrm{d}t} = \frac{\partial}{\partial t} + \gamma_E x\frac{\partial}{\partial y} + \frac{\rho_e v_{\mathrm{the}}}{2}\left(\boldsymbol{z}\times\boldsymbol{\nabla}\varphi\right)\cdot\boldsymbol{\nabla} + \nu\nabla_\perp^4. \tag{36}$$

Why this model?

Fluid slab ETG model

We performed numerical simulations of the following collisional ETG model (first studied by Adkins et al., 2023)

$$\frac{\mathrm{d}}{\mathrm{d}t}\frac{\delta n_e}{n_{0e}} + \frac{\partial u_{\parallel e}}{\partial z} = 0, \tag{33}$$

$$\frac{\mathrm{d}}{\mathrm{d}t}\frac{\delta T_e}{T_{0e}} - \frac{c_3 v_{\mathrm{th}e}^2}{3\nu_{ei}}\frac{\partial^2}{\partial z^2}\frac{\delta T_e}{T_{0e}} + \frac{2}{3}\left(1+\frac{c_2}{c_1}\right)\frac{\partial u_{\parallel e}}{\partial z} = -\frac{\rho_e v_{\mathrm{th}e}}{2L_T}\frac{\partial \varphi}{\partial y}, \tag{34}$$

where $\varphi = e\phi/T_{0e}$,

$$\frac{\nu_{ei}}{c_1}\frac{u_{\parallel e}}{v_{\mathrm{th}e}} = -\frac{v_{\mathrm{th}e}}{2}\frac{\partial}{\partial z}\left[\frac{\delta n_e}{n_{0e}} - \varphi + \left(1+\frac{c_2}{c_1}\right)\frac{\delta T_e}{T_{0e}}\right], \tag{35}$$

and

$$\frac{\mathrm{d}}{\mathrm{d}t} = \frac{\partial}{\partial t} + \gamma_E x \frac{\partial}{\partial y} + \frac{\rho_e v_{\mathrm{th}e}}{2}\left(\boldsymbol{z}\times\boldsymbol{\nabla}\varphi\right)\cdot\boldsymbol{\nabla} + \nu\nabla_\perp^4. \tag{36}$$

Why this model?

Because it agrees remarkably well with a critically balanced free-energy cascade!

Fluid slab ETG model (no flow shear)

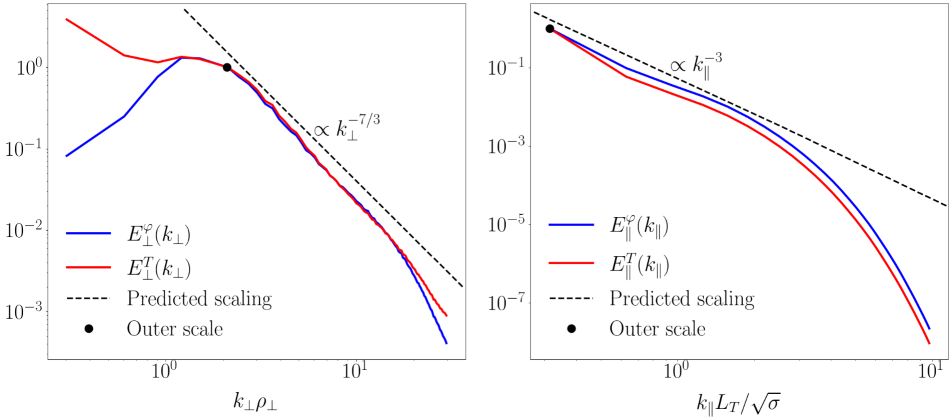

Figure 1: Numerical spectra and theoretical predictions (Adkins et al. 2023).

Fluid slab ETG model (no flow shear)

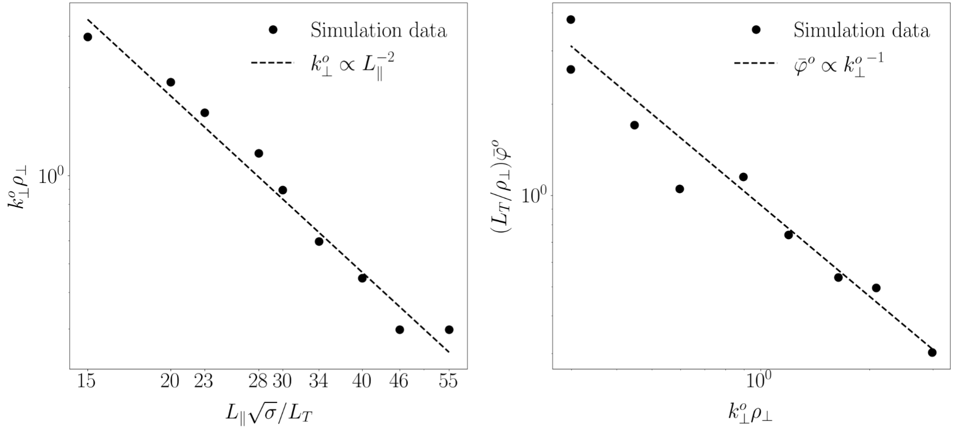

Figure 2: Outer scale and theoretical predictions (Adkins et al. 2023).

Fluid slab ETG model (no flow shear)

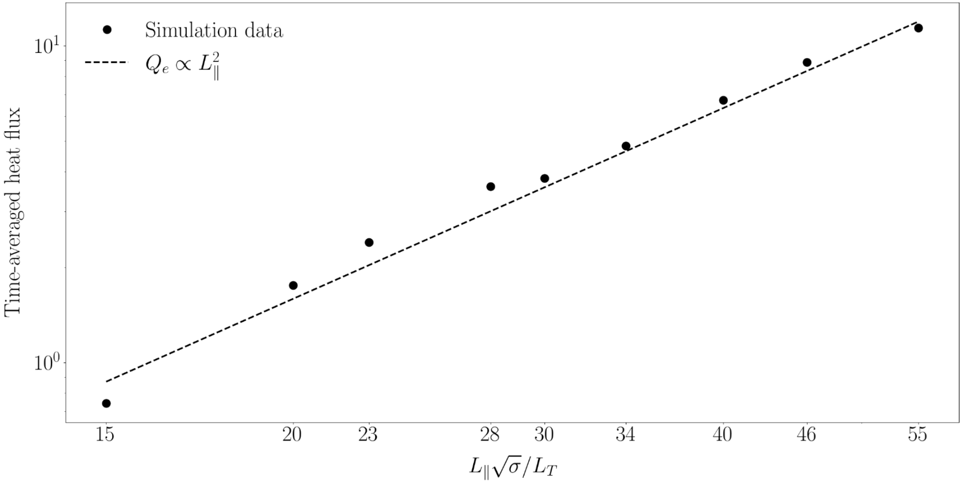

Figure 3: Heat flux and theoretical predictions (Adkins et al. 2023).

Fluid slab ETG model

If our theory has any hopes of working anywhere, it better work in this model...

Flow shear in the fluid model

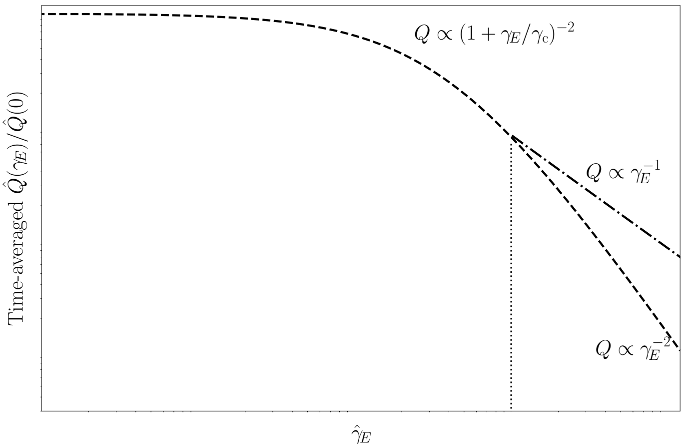

Flow shear in the fluid model

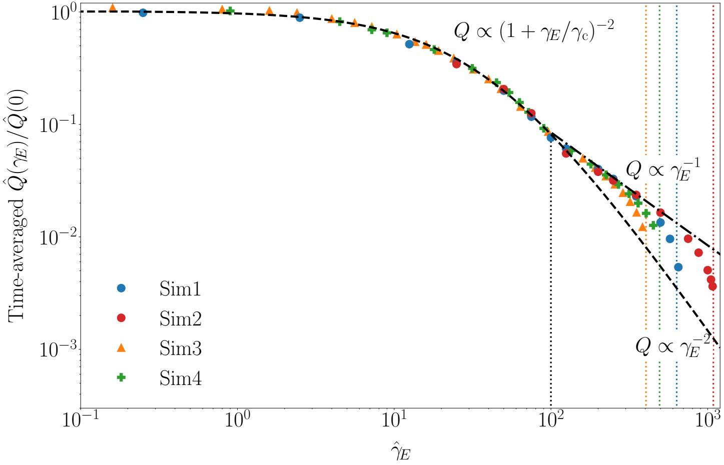

Flow shear in the fluid model

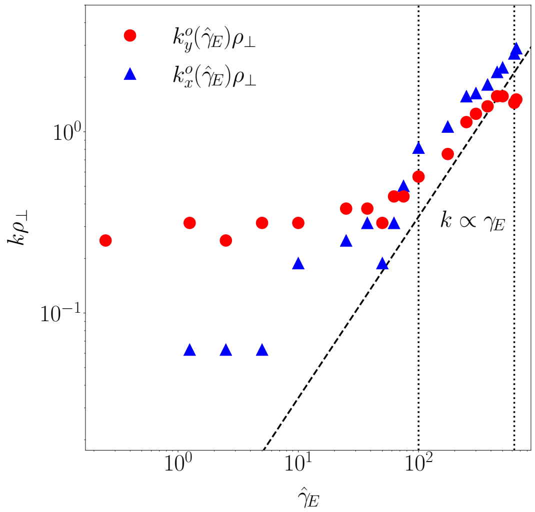

Flow shear in the fluid model

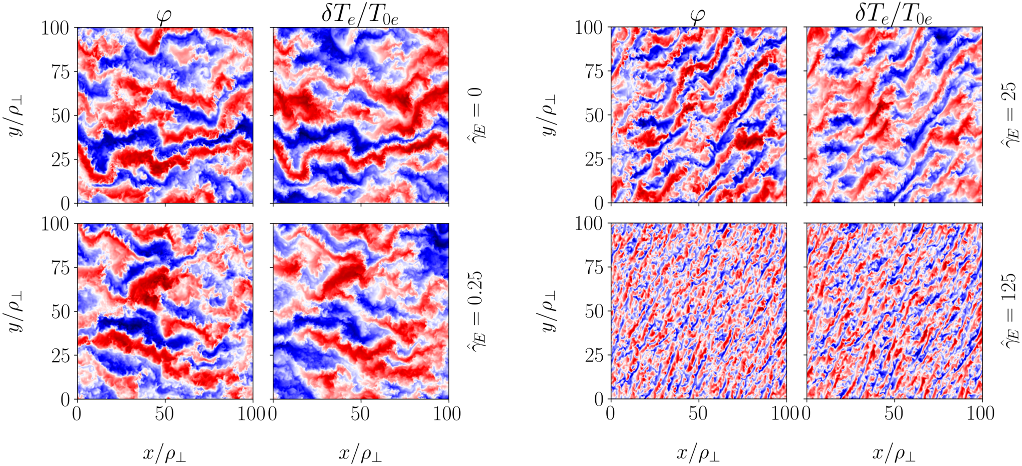

Flow shear in the fluid model

Flow shear in the fluid model

- We find $\mathcal{A}^{\circ}(0) \approx 0.3$, consistent with the $O(10)$ suppression of the heat flux in the weakly sheared regime.

Flow shear in the fluid model

- We find $\mathcal{A}^{\mathrm{o}}(0) \approx 0.3$, consistent with the $O(10)$ suppression of the heat flux in the weakly sheared regime.
- The numerical data suggests (in normalised units) $\hat{\gamma}^{\mathrm{o}} \approx 100$ and $\hat{\gamma}_{\mathrm{c}} \approx 40$, consistent with $\mathcal{A}^{\mathrm{o}}(0) \approx 0.3$.

Flow shear in the fluid model

- We find $\mathcal{A}^{\mathrm{o}}(0) \approx 0.3$, consistent with the $O(10)$ suppression of the heat flux in the weakly sheared regime.
- The numerical data suggests (in normalised units) $\hat{\gamma}^{\mathrm{o}} \approx 100$ and $\hat{\gamma}_{\mathrm{c}} \approx 40$, consistent with $\mathcal{A}^{\mathrm{o}}(0) \approx 0.3$.
- Very good agreement between the theory and the relevant observables, e.g., $k_x^{\mathrm{o}}(\gamma_E), k_y^{\mathrm{o}}(\gamma_E), Q(\gamma_E)$.

Flow shear in the fluid model

- We find $\mathcal{A}^{\mathrm{o}}(0) \approx 0.3$, consistent with the $O(10)$ suppression of the heat flux in the weakly sheared regime.
- The numerical data suggests (in normalised units) $\hat{\gamma}^{\mathrm{o}} \approx 100$ and $\hat{\gamma}_{\mathrm{c}} \approx 40$, consistent with $\mathcal{A}^{\mathrm{o}}(0) \approx 0.3$.
- Very good agreement between the theory and the relevant observables, e.g., $k_x^{\mathrm{o}}(\gamma_E), k_y^{\mathrm{o}}(\gamma_E), Q(\gamma_E)$.

Theory looks good! Let's go to GK...

GK results

- **GENE** simulations for a γ_E scan (PVG is off!) of ITG turbulence in a Cyclone-base-case equilibrium with $\hat{s} = 0.796$, $q_0 = 1.4$, $\epsilon = 0.18$, $k_{x,\min}\rho_i = 1.6 \times 10^{-2}$, $k_{y,\min}\rho_i = 6.25 \times 10^{-3}$, $n_x = 288$, $n_z = 16$, $n_v = 32$, $n_\mu = 8$.

GK results

- `GENE` simulations for a γ_E scan (PVG is off!) of ITG turbulence in a Cyclone-base-case equilibrium with $\hat{s} = 0.796$, $q_0 = 1.4$, $\epsilon = 0.18$, $k_{x,\min}\rho_i = 1.6 \times 10^{-2}$, $k_{y,\min}\rho_i = 6.25 \times 10^{-3}$, $n_x = 288$, $n_z = 16$, $n_v = 32$, $n_\mu = 8$.
- Two different temperature gradients: $R/L_T = 10, n_y = 256$ and $R/L_T = 14, n_y = 512$.

GK results

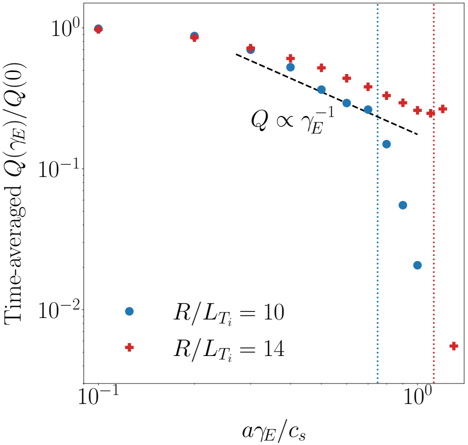

Time-averaged $Q(\gamma_E)/Q(0)$
10^0
10^{-1}
10^{-2}
10^{-1}
10^0
$a\gamma_E/c_s$
$Q \propto \gamma_E^{-1}$
$R/L_{T_i} = 10$
$R/L_{T_i} = 14$

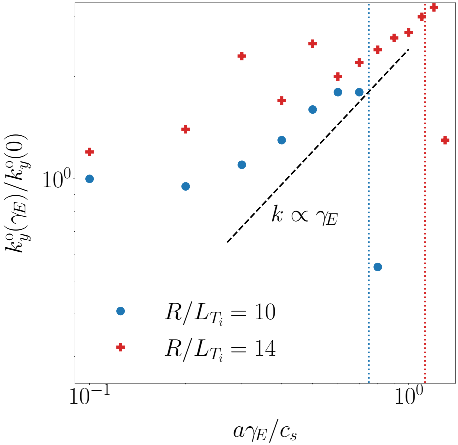

$k_y^o(\gamma_E)/k_y^o(0)$
10^0
10^{-1}
10^0
$a\gamma_E/c_s$
$k \propto \gamma_E$
$R/L_{T_i} = 10$
$R/L_{T_i} = 14$

GK results

- The ion-temperature-gradient-driven turbulence we simulated has $\mathcal{A}^{\mathrm{o}}(0) \sim 1$, so no clear weakly sheared regime.

GK results

- The ion-temperature-gradient-driven turbulence we simulated has $\mathcal{A}^{\mathrm{o}}(0) \sim 1$, so no clear weakly sheared regime.
- Has a well-defined strongly sheared regime that ends at $\gamma_E \approx 1.5\gamma_{\max}$.

GK results

- The ion-temperature-gradient-driven turbulence we simulated has $\mathcal{A}^{\mathrm{o}}(0) \sim 1$, so no clear weakly sheared regime.
- Has a well-defined strongly sheared regime that ends at $\gamma_E \approx 1.5\gamma_{\max}$.

Very reasonable agreement with GK!

Before we move on...

... a quick teaser of the interesting physics of the marginal state.

Teaser: marginal regime in the fluid model

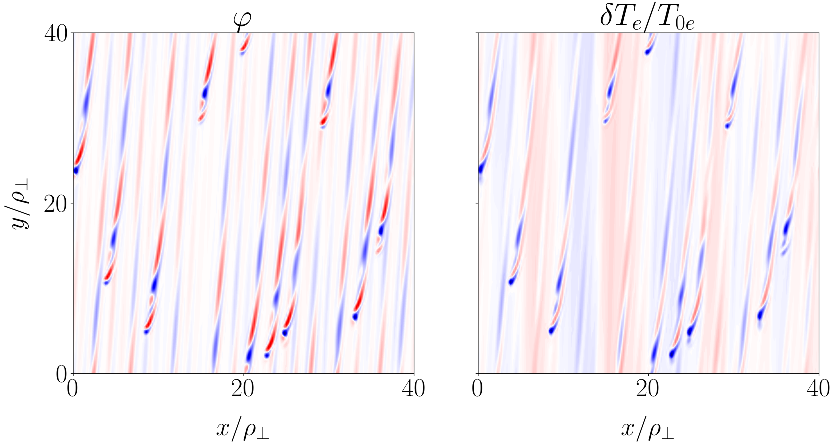

Figure 4: Radial localisation of turbulent perturbations at very large values of flow shear.

Readily happens in other fluid models, too...

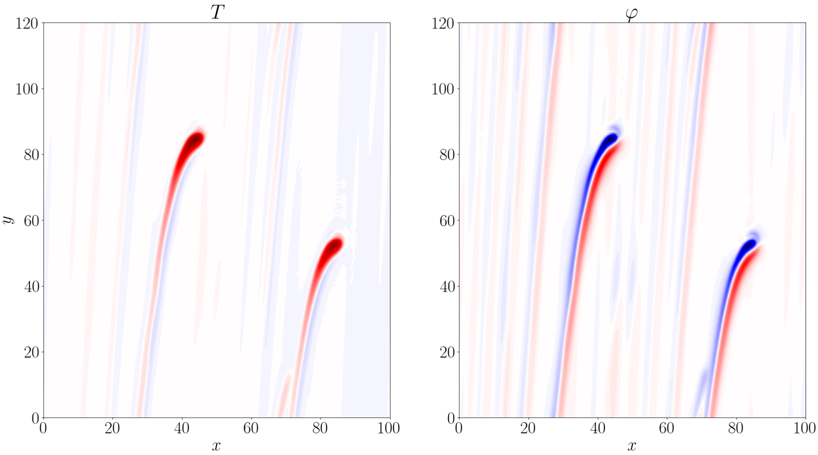

Figure 5: Radial localisation of turbulent perturbations at very large values of flow shear **in a completely different ion-scale model of curvature-driven turbulence**.

Teaser: marginal regime in GK ($R/L_{T_i} = 14$)

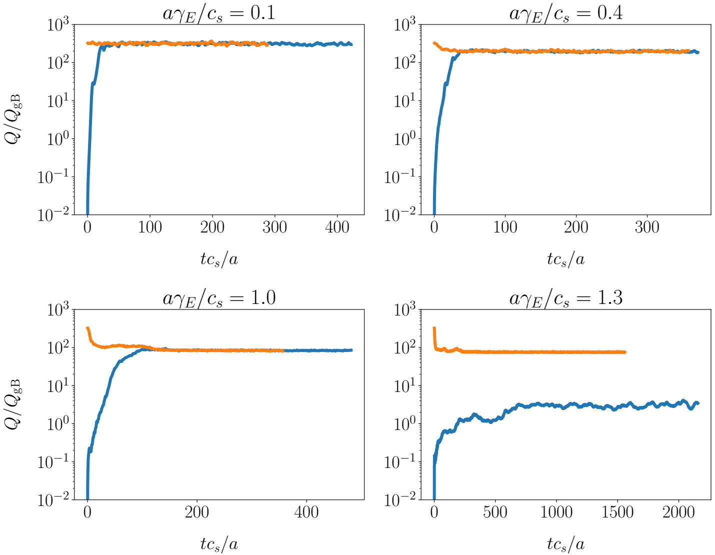

Outline

Cross-scale interactions in GK

- Numerical and experimental evidence points towards turbulence at two disparate scales: ρ_e and ρ_i, with $\rho_e/\rho_i \sim \sqrt{m_e/m_i} \ll 1$.

Cross-scale interactions in GK

- Numerical and experimental evidence points towards turbulence at two disparate scales: ρ_e and ρ_i, with $\rho_e/\rho_i \sim \sqrt{m_e/m_i} \ll 1$.
- Under the GK ordering $\gamma_s \sim v_{\mathrm{th}s}/L$, and so $\gamma_e/\gamma_i \sim \sqrt{m_i/m_e} \gg 1$.

Cross-scale interactions in GK

- Numerical and experimental evidence points towards turbulence at two disparate scales: ρ_e and ρ_i, with $\rho_e/\rho_i \sim \sqrt{m_e/m_i} \ll 1$.
- Under the GK ordering $\gamma_s \sim v_{\mathrm{th}s}/L$, and so $\gamma_e/\gamma_i \sim \sqrt{m_i/m_e} \gg 1$.

How do the slow, large-scale ion fluctuations interact with the fast, small-scale electron ones?

Cross-scale interactions in GK

- Numerical and experimental evidence points towards turbulence at two disparate scales: ρ_e and ρ_i, with $\rho_e/\rho_i \sim \sqrt{m_e/m_i} \ll 1$.
- Under the GK ordering $\gamma_s \sim v_{\mathrm{th}s}/L$, and so $\gamma_e/\gamma_i \sim \sqrt{m_i/m_e} \gg 1$.

How do the slow, large-scale ion fluctuations interact with the fast, small-scale electron ones?

- Simulations and experiments suggest that ion fluctuations can suppress the electron ones (Candy et al., 2007; Waltz et al., 2007; Maeyama et al., 2015; Howard et al., 2016a,b).

Cross-scale interactions in GK

- Numerical and experimental evidence points towards turbulence at two disparate scales: ρ_e and ρ_i, with $\rho_e/\rho_i \sim \sqrt{m_e/m_i} \ll 1$.
- Under the GK ordering $\gamma_s \sim v_{\mathrm{th}s}/L$, and so $\gamma_e/\gamma_i \sim \sqrt{m_i/m_e} \gg 1$.

How do the slow, large-scale ion fluctuations interact with the fast, small-scale electron ones?

- Simulations and experiments suggest that ion fluctuations can suppress the electron ones (Candy et al., 2007; Waltz et al., 2007; Maeyama et al., 2015; Howard et al., 2016a,b).

Could this be as simple as ion-scale flows shearing electron-scale eddies?

Cross-scale interactions in GK

- Numerical and experimental evidence points towards turbulence at two disparate scales: ρ_e and ρ_i, with $\rho_e/\rho_i \sim \sqrt{m_e/m_i} \ll 1$.
- Under the GK ordering $\gamma_s \sim v_{\mathrm{th}s}/L$, and so $\gamma_e/\gamma_i \sim \sqrt{m_i/m_e} \gg 1$.

How do the slow, large-scale ion fluctuations interact with the fast, small-scale electron ones?

- Simulations and experiments suggest that ion fluctuations can suppress the electron ones (Candy et al., 2007; Waltz et al., 2007; Maeyama et al., 2015; Howard et al., 2016a,b).

Could this be as simple as ion-scale flows shearing electron-scale eddies?

- Naïvely, the quench rule suggests that this cannot happen in a scale-separated way: ion-scale fluctuating shear is $\gamma_{E,i} \sim \gamma_i$, but electron-scale instabilities grow at $\gamma_e \gg \gamma_i$.

Cross-scale interactions in GK

- Numerical and experimental evidence points towards turbulence at two disparate scales: ρ_e and ρ_i, with $\rho_e/\rho_i \sim \sqrt{m_e/m_i} \ll 1$.
- Under the GK ordering $\gamma_s \sim v_{\mathrm{th}s}/L$, and so $\gamma_e/\gamma_i \sim \sqrt{m_i/m_e} \gg 1$.

How do the slow, large-scale ion fluctuations interact with the fast, small-scale electron ones?

- Simulations and experiments suggest that ion fluctuations can suppress the electron ones (Candy et al., 2007; Waltz et al., 2007; Maeyama et al., 2015; Howard et al., 2016a,b).

Could this be as simple as ion-scale flows shearing electron-scale eddies?

- Naïvely, the quench rule suggests that this cannot happen in a scale-separated way: ion-scale fluctuating shear is $\gamma_{E,i} \sim \gamma_i$, but electron-scale instabilities grow at $\gamma_e \gg \gamma_i$.
- Indeed, it may not be perpendicular shear at all (Hardman et al., 2019; Hardman et al., 2020).

Cross-scale interactions in GK

- However, electron-scale fluctuations are often found to be highly elongated in the radial direction (streamers).

Cross-scale interactions in GK

- However, electron-scale fluctuations are often found to be highly elongated in the radial direction (streamers).
- If their radial size is $\sim \rho_i$, the ion-scale fluctuating flow shear falls right in the weakly sheared regime $\gamma_{\mathrm{c},e} \sim \gamma_i$.

Cross-scale interactions in GK

- However, electron-scale fluctuations are often found to be highly elongated in the radial direction (streamers).
- If their radial size is $\sim \rho_i$, the ion-scale fluctuating flow shear falls right in the weakly sheared regime $\gamma_{\mathrm{c},e} \sim \gamma_i$.
- In that regime, the electron-scale transport is highly sensitive to the ion-scale flow shear, viz., $Q_e \propto \gamma_{E,i}^{-2}$

Cross-scale interactions in GK

- However, electron-scale fluctuations are often found to be highly elongated in the radial direction (streamers).
- If their radial size is $\sim \rho_i$, the ion-scale fluctuating flow shear falls right in the weakly sheared regime $\gamma_{\mathrm{c},e} \sim \gamma_i$.
- In that regime, the electron-scale transport is highly sensitive to the ion-scale flow shear, viz., $Q_e \propto \gamma_{E,i}^{-2}$

Scale-separated asymptotic theory of cross-scale interactions?

Cross-scale interactions in GK

- However, electron-scale fluctuations are often found to be highly elongated in the radial direction (streamers).
- If their radial size is $\sim \rho_i$, the ion-scale fluctuating flow shear falls right in the weakly sheared regime $\gamma_{\mathrm{c},e} \sim \gamma_i$.
- In that regime, the electron-scale transport is highly sensitive to the ion-scale flow shear, viz., $Q_e \propto \gamma_{E,i}^{-2}$

Scale-separated asymptotic theory of cross-scale interactions?

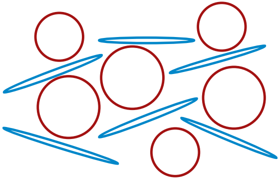

Summary

- We have extended the phenomenological theory of saturation of turbulence via a direct local energy cascade to include the effects of perpendicular flow shear.

Summary

- We have extended the phenomenological theory of saturation of turbulence via a direct local energy cascade to include the effects of perpendicular flow shear.
- We have identified two regimes:

Summary

- We have extended the phenomenological theory of saturation of turbulence via a direct local energy cascade to include the effects of perpendicular flow shear.
- We have identified two regimes:
  (i) weak-shear regime (‘shearing rate smaller than intrinsic turbulent rate’),

Summary

- We have extended the phenomenological theory of saturation of turbulence via a direct local energy cascade to include the effects of perpendicular flow shear.
- We have identified two regimes:
  (i) weak-shear regime ('shearing rate smaller than intrinsic turbulent rate'),
  (ii) strong-shear regime ('shearing rate larger than intrinsic turbulent rate').

Summary

- We have extended the phenomenological theory of saturation of turbulence via a direct local energy cascade to include the effects of perpendicular flow shear.
- We have identified two regimes:
  (i) weak-shear regime ('shearing rate smaller than intrinsic turbulent rate'),
  (ii) strong-shear regime ('shearing rate larger than intrinsic turbulent rate').
- **Streamer-dominated turbulence is heavily suppressed by weak flow shear.**

Summary

- We have extended the phenomenological theory of saturation of turbulence via a direct local energy cascade to include the effects of perpendicular flow shear.
- We have identified two regimes:
  (i) weak-shear regime ('shearing rate smaller than intrinsic turbulent rate'),
  (ii) strong-shear regime ('shearing rate larger than intrinsic turbulent rate').
- **Streamer-dominated turbulence is heavily suppressed by weak flow shear.**
- Theory agrees remarkably well with simulations.

Summary

- We have extended the phenomenological theory of saturation of turbulence via a direct local energy cascade to include the effects of perpendicular flow shear.
- We have identified two regimes:
  (i) weak-shear regime ('shearing rate smaller than intrinsic turbulent rate'),
  (ii) strong-shear regime ('shearing rate larger than intrinsic turbulent rate').
- **Streamer-dominated turbulence is heavily suppressed by weak flow shear.**
- Theory agrees remarkably well with simulations.

Apart from bringing us theoretical enlightenment, this theory could be crucial for understanding cross-scale interactions.

Backup slides

Details be here

Fluctuations at a given scale

$$\overline{\varphi}^2 \equiv \int_{|k'_y|>k_y} \mathrm{d}k'_y \int_{-\infty}^{+\infty} \mathrm{d}k'_x \int \frac{\mathrm{d}z}{L_\parallel} \, |\varphi_{\boldsymbol{k'}_\perp}|^2, \tag{37}$$

Fluid model

Derived for

$$k_\parallel L_T \sim \sqrt{\sigma}, \quad k_\perp \rho_\perp \sim 1, \quad \rho_\perp \equiv \frac{\rho_e}{\sigma}\frac{L_T}{\lambda_{ei}}, \tag{38}$$

$$\beta_e \ll \sigma \ll 1. \tag{39}$$

The normalised heat flux and flow shear are

$$\hat{Q} \equiv \left(\frac{L_T}{L_\parallel \sqrt{\sigma}}\right)^2 \frac{Q}{(\rho_\perp/\rho_e) Q_{\mathrm{gB}e}}, \tag{40}$$

$$\hat{\gamma}_E \equiv \left(\frac{L_T}{L_\parallel \sqrt{\sigma}}\right)^{-2} \frac{\gamma_E}{\omega_\perp}, \tag{41}$$

where $\omega_\perp = \rho_e v_{\mathrm{th}e}/2\rho_\perp L_T$.

Fluid simulations

	$L_\perp/\rho_\perp$	$L_\parallel\sqrt{\sigma}/L_T$	$n_\perp$	$n_\parallel$	$\nu_\perp\rho_e^4/\omega_\perp\rho_\perp^4$	$\hat{\gamma}_{\max}$
Sim1	100	50	341	31	5×10^{-4}	6.3×10^{2}
Sim2	100	50	683	31	2.5×10^{-5}	1.7×10^{3}
Sim3	70	40	191	31	5×10^{-4}	4.1×10^{2}
Sim4	40	30	191	31	5×10^{-5}	4.9×10^{2}

Table 1: A summary of the simulation parameters for the fluid simulations. The simulation domain is taken to be 'square' with $L_x = L_y = L_\perp$ and $n_x = n_y = n_\perp$, where n_x, n_y, and $n_\parallel$ are the number of resolved (i.e., dealiased) Fourier modes in the x, y, and z coordinates, respectively. The last column shows the maximum growth rate $\gamma_{\max}$ normalized as (41).

Inertial transition region

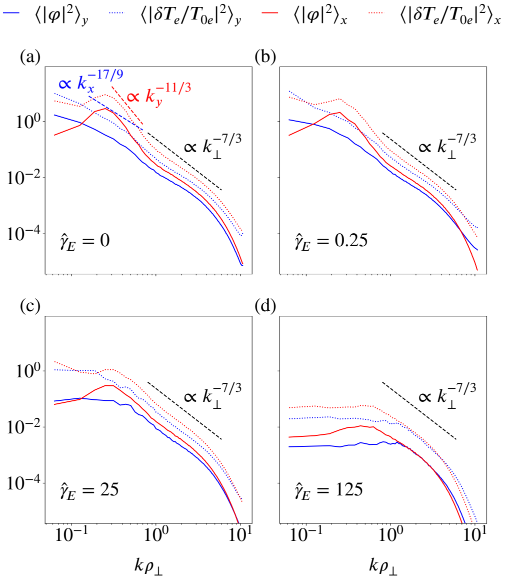

Minimal model for ITG ferdinons

- Ferdinons are captured by the following one-parameter minimal model:

$$(\partial_t + Sx\partial_y)\,\varphi - \partial_y T = \nabla_\perp^2\varphi, \tag{42}$$

$$(\partial_t + Sx\partial_y)\,T + \partial_y\varphi' + \{\varphi, T\} = \nabla_\perp^2 T, \tag{43}$$

where

$$S = \frac{\gamma_E \chi}{\kappa_T}. \tag{44}$$

- **Numerically, ferdinons survive only for $S \in [0.172, 0.176]$!**
- Suggests a unique S for an infinite-life-time ferdinon?

Adkins, T., Ivanov, P. G. & Schekochihin, A. A. 2023 Scale invariance and critical balance in electrostatic drift-kinetic turbulence. *J. Plasma Phys.* **89**, 905890406.

Barnes, M., Parra, F. I. & Schekochihin, A. A. 2011 Critically balanced ion temperature gradient turbulence in fusion plasmas. *Phys. Rev. Lett.* **107**, 115003.

Candy, J., Waltz, R. E., Fahey, M. R. & Holland, C. 2007 The effect of ion-scale dynamics on electron-temperature-gradient turbulence. *Plasma Phys. Control. Fusion* **49**, 1209.

Ghim, Y.-c., Schekochihin, A. A., Field, A. R., Abel, I. G., Barnes, M., Colyer, G., Cowley, S. C., Parra, F. I., Dunai, D. & Zoletnik, S. 2013 Experimental signatures of critically balanced turbulence in MAST. *Phys. Rev. Lett.* **110**, 145002.

Goldreich, P. & Sridhar, S. 1995 Toward a theory of interstellar turbulence. 2: Strong Alfvénic turbulence. *Astrophys. J.* **438**, 763.

Hardman, M. R., Barnes, M. & Roach, C. M. 2020 Stabilisation of short-wavelength instabilities by parallel-to-the-field shear in long-wavelength $E \times B$ flows. *J. Plasma Phys.* **86**, 905860601.

Hardman, M. R., Barnes, M., Roach, C. M. & Parra, F. I. 2019 A scale-separated approach for studying coupled ion and electron scale turbulence. *Plasma Phys. Control. Fusion* **61** (6), 065025, arXiv: 1901.07062.

Howard, N. T., Holland, C., White, A. E., Greenwald, M. & Candy, J. 2016a Multi-scale gyrokinetic simulation of tokamak plasmas: enhanced heat loss due to cross-scale coupling of plasma turbulence. *Nuclear Fusion* **56** (1), 014004.

Howard, N. T., Holland, C., White, A. E., Greenwald, M., Candy, J. & Creely, A. J. 2016b Multi-scale gyrokinetic simulations: Comparison with experiment and implications for predicting turbulence and transport. *Physics of Plasmas* **23** (5), 056109.

Kolmogorov, A. N. 1941 Local structure of turbulence in incompressible viscous fluid at very large Reynolds numbers. *Dokl. Acad. Nauk SSSR* **30**, 299.

Maeyama, S., Idomura, Y., Watanabe, T. H., Nakata, M., Yagi, M., Miyato, N., Ishizawa, A. & Nunami, M. 2015 Cross-Scale Interactions between Electron and Ion Scale Turbulence in a Tokamak Plasma. *Phys. Rev. Lett.* **114** (25), 255002.

Nies, R., Parra, F. I., Barnes, M., Mandell, N. & Dorland, W. 2023 Radial magnetic drift effects on critical balance and secondary instability. In 14$^{\text{th}}$ Plasma Kinetics Working Meeting, WPI, Vienna.

Waltz, R. E., Candy, J. & Fahey, M. 2007 Coupled ion temperature gradient and trapped electron mode to electron temperature gradient mode gyrokinetic simulationsa). *Phys. Plasmas* **14**, 056116.

Waltz, R. E., Dewar, R. L. & Garbet, X. 1998 Theory and simulation of rotational shear stabilization of turbulence. *Phys. Plasmas* **5**, 1784.